ELECTRO-OPTICAL SYSTEMS, INC.
A XEROX COMPANY
PASADENA, CALIFORNIA 91107 • 213/351-2351

Second Quarterly Progress Report

THERMIONIC RESEARCH AND DEVELOPMENT PROGRAM

Prepared for
Jet Propulsion Laboratory
California Institute of Technology
4800 Oak Grove Drive
Pasadena, California
Attention: J. M. Skipton

Contract 952217

EOS Report 4006-Q-2 12 October 1968

Prepared by
D. L. Jacobson
R. Hamerdinger
A. Campbell

Approved by

A. O. Jensen, Manager
Electro-Optical and Solid State Technology Division

ELECTRO-OPTICAL SYSTEMS, INC.
A XEROX COMPANY

This work was performed for the Jet Propulsion Laboratory, California Institute of Technology, sponsored by the National Aeronautics and Space Administration under Contract NAS7-100.

CONTENTS

ILLUSTRATIONS

ILLUSTRATIONS (contd)

SECTION 1

INTRODUCTION

The work described in this, the second quarterly progress report, is being performed under JPL Contract 952217, a 12-month, three-task program of advanced thermionic converter development.

The first task consists of an investigation of single crystal rhenium electrodes or other refractory materials for the purpose of yielding a low work function collector surface. Specific investigations include vacuum emission vehicle determination of the effective and Richardson work functions as well as qualitative and quantitative examination of electrode surfaces using a thermionic emission microscope. Metallurgical examinations include X-ray diffraction and metallographic and spectrographic analyses. These same electrodes will then be investigated in a variable parameter test vehicle for minimum work function and optimized power output. Based upon variable parameter test vehicle data, a planar converter will be fabricated and tested for the purpose of comparing test vehicle to converter performance.

Task II consists of the investigation of vapor-deposited tungsten 20-percent rhenium alloy electrodes in the same manner as in Task I, i.e., utilizing vacuum emission, electron emission microscope, and variable parameter vehicle evaluations with, however, the subsequent fabrication and testing of two planar converters.

Task III completes the program effort with the design, fabrication, and test of cylindrical thermionic converters for the principal purpose of providing a direct performance comparison between planar and cylindrical converters.

The cylindrical converter design is adaptable to radioisotopic and out-of-file thermionic systems. Basically, the design allows the individual converter to be mounted on a sapphire insulated heat-pipe emanating from a common heat source to form an array of converters that can be externally connected for series-parallel choice hook-up. Moreover, each converter contains a separate reservoir which allows for individual converter testing and optimization.

An array of five converters could yield an estimated electrical output of 100 watts at 2.0 volts; ten such arrays could yield an unconditioned electrical power output of 1 kilowatt.

SECTION 2

ELECTRODE MATERIALS EVALUATION (TASK I)

2.1 POLYCRYSTALLINE RHENIUM ELECTRODE VARIABLE PARAMETER VEHICLE

The polycrystalline rhenium electrode variable parameter test vehicle built for JPL under contract 951225 was reinstalled in a test station at EOS for additional investigation. The first requirement was to compare the output performance with that previously achieved. This was accomplished by reproducing the curve showing the variation of voltage output with interelectrode spacing at a constant current of 38 amperes, an emitter temperature of 1735°C true hohlraum, a collector temperature of 704°C and a cesium reservoir temperature of 331°C (Pressure = 4.04 torr). Figure 1 is a comparison of the curve produced under JPL Contract 951225 and on the present contract, indicating the consistency of the data. The voltage at maximum power output from the earlier work is approximately 0.8 volts at an interelectrode spacing of 0.0038 in., or at 15.35 mil-torr. The voltage at maximum power output from the present work is 0.79 volts at 0.004 in., or at 15.72 mil-torr.

Performance characteristics are shown in Figures 2 and 3 at other operating conditions, specifically at lower emitter temperatures, the work being done under the present contract. Figure 2 shows the variation of voltage output with interelectrode spacing at an emitter temperature of 1530°C true hohlraum, a cesium reservoir of 321°C, a collector temperature of 715°C and a constant current level of 45.7 amperes. The maximum voltage output is 0.435 volts at an interelectrode spacing of 0.0047 in., or at 14.85 mil-torr. Figure 3 shows the performance characteristic with an emitter temperature of 1425°C, a cesium

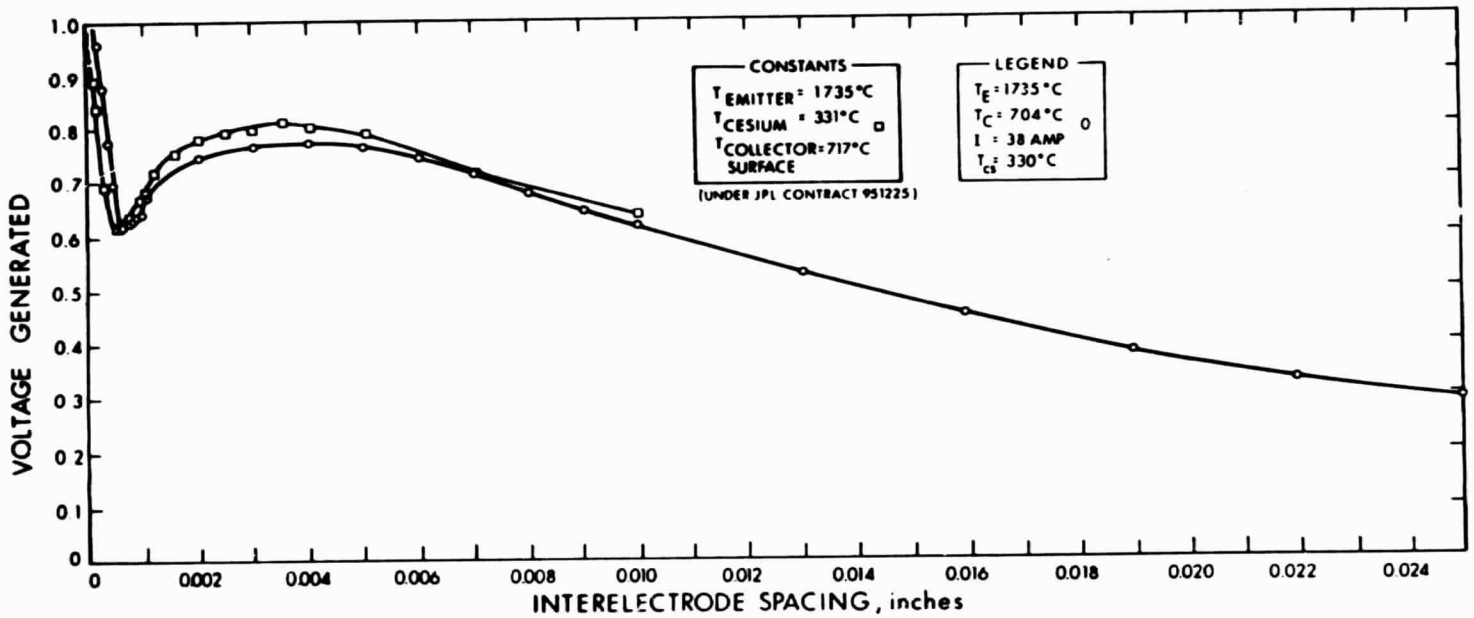

Figure 1. Interelectrode Spacing versus Voltage. Emitter, Collector, and Cesium Reservoir Temperature Constant (all dc data points).

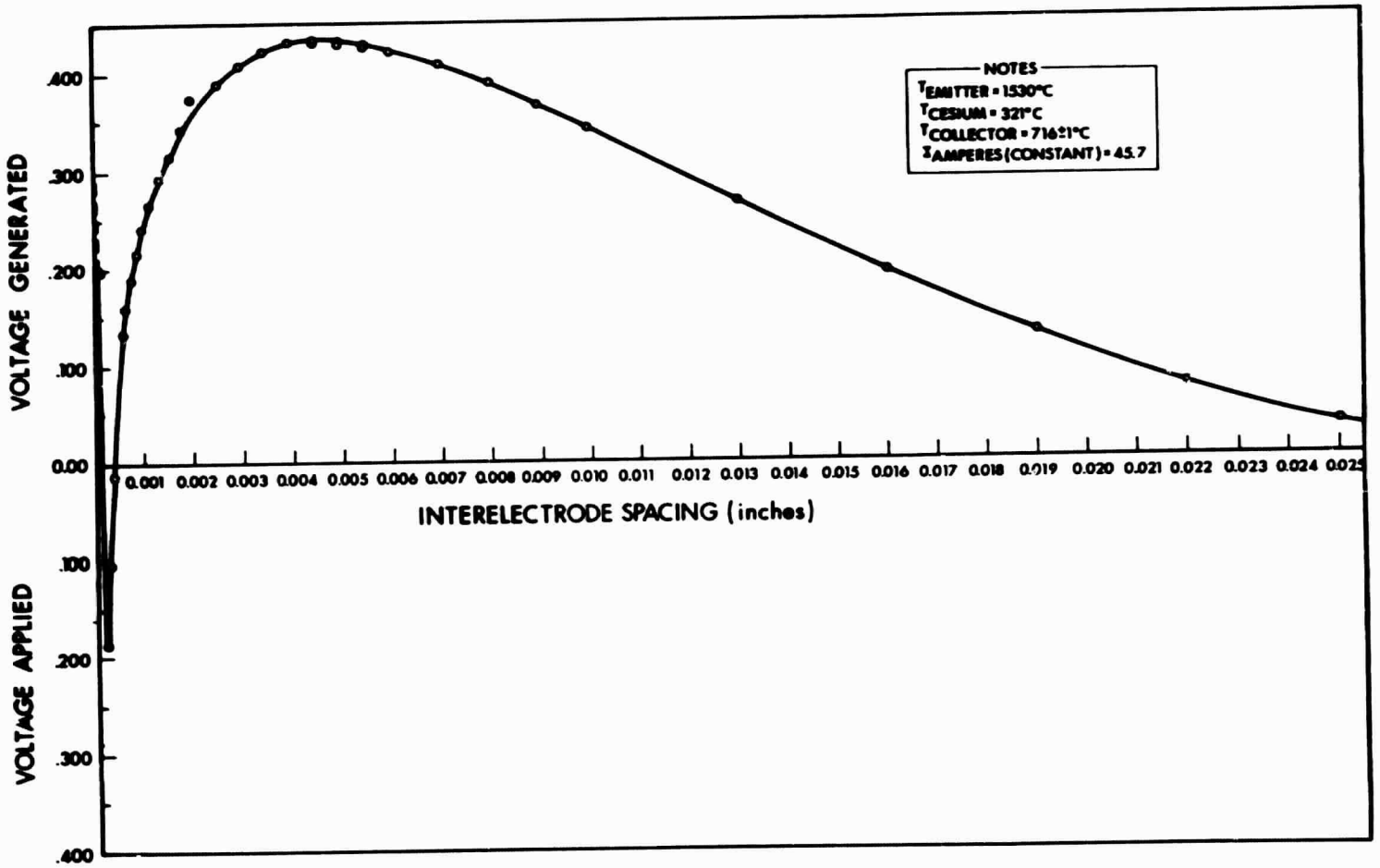

Figure 2. Interelectrode Spacing versus Voltage. Collector, and Cesium Reservoir Temperature Constant (all dc data points)

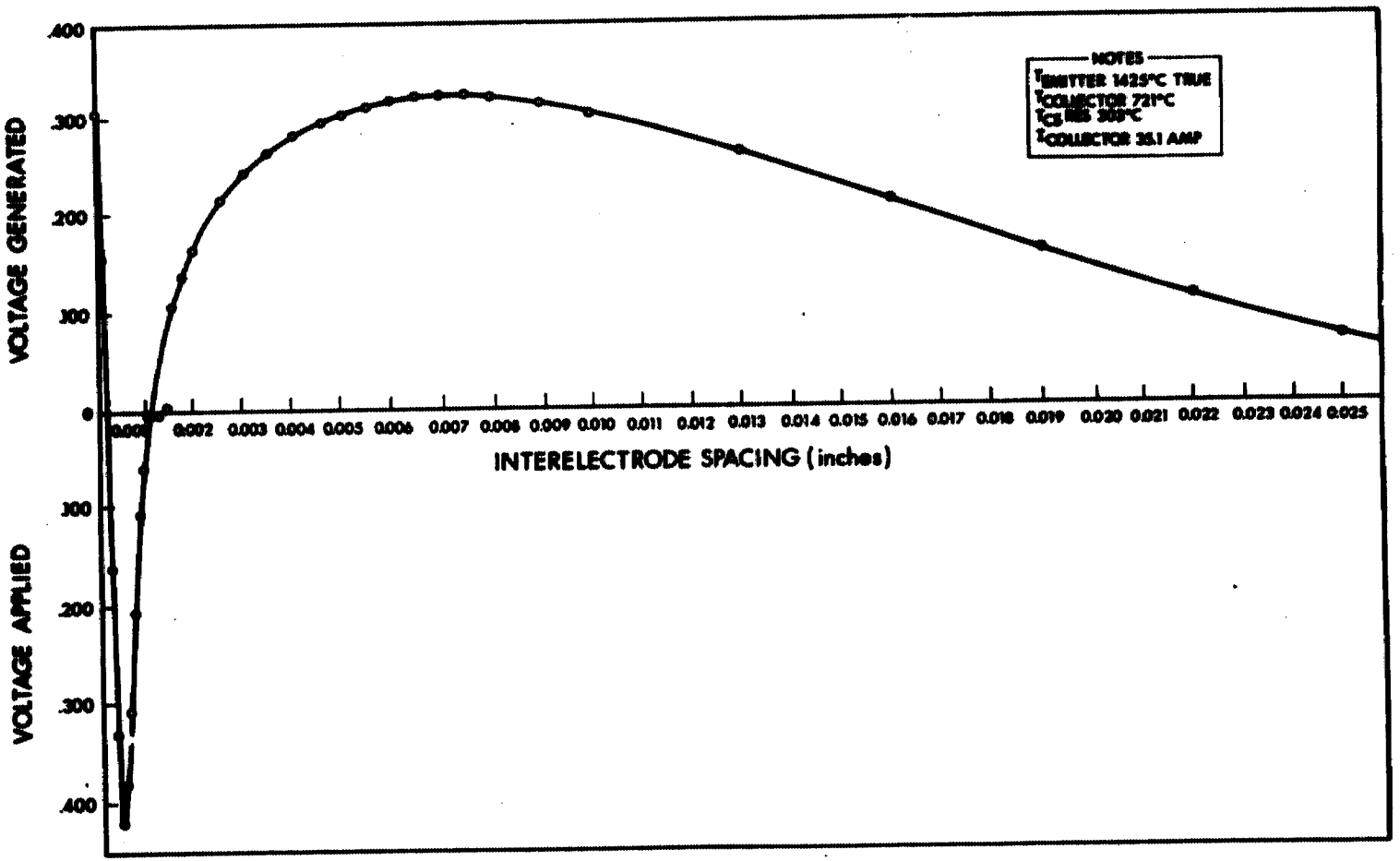

Figure 3. Interelectrode Spacing versus Emitter, Collector, and Cesium Reservoir Temperature Constant (all dc)

reservoir temperature of 303°C, a collector temperature of 721°C and a constant current of 35.1 amperes. The voltage at maximum power output is 0.325 volts at an interelectrode spacing of 0.0075 in., or at 15.3 mil-torr.

The results of Figures 1 and 3 show that the pressure-distance relationship for maximum voltage output at constant current holds to within ±0.8 mill-torr of 16 mil-torr previously exhibited experimentally by EOS. Figure 2 exhibits a slightly lower value possibly resulting from thermocouple placement with respect to the true cesium liquid-vapor interface within the reservoir tubulation. Langmuir's equation for the determination of cesium vapor pressure associated with a particular reservoir temperature was used and is given as follows:

$$\log_{10} P_{mm} = 11.0531 - 1.35 \log_{10} T_{oK} - \frac{4041}{T_{oK}}.$$

Cesiated work function measurements (Langmuir "S" curves) from the polycrystalline rhenium electrode system were produced for pressures of 3.83, 2.66, 1.39, 0.50, 0.20, and 0.05 torr in Figure 4. In all of the work function measurements, the volt-ampere characteristics were obtained by the combined dc and ac method, tracing an instantaneous characteristic at fixed parameter temperatures. The I-V characteristic is swept out about the dc point keeping the emitter temperature constant. Collector current is determined by measuring the voltage drop across a calibrated 0.1 percent shunt and displayed on the y-axis of an oscilloscope. A 10 volt, 100 ampere Kepco power supply with a programmed internal sweep was used where the required current level permitted. Otherwise, a low inductance, low impedance, secondary stepdown transformer was employed as a sweep source with a resistive load across the test vehicle. A Sorenson power supply was used to sustain the current level in the guard ring in proportion to the collecting area difference between collector and guard ring. During the sweep, the guard ring-emitter sweep maintained the same proportion. The saturated emission

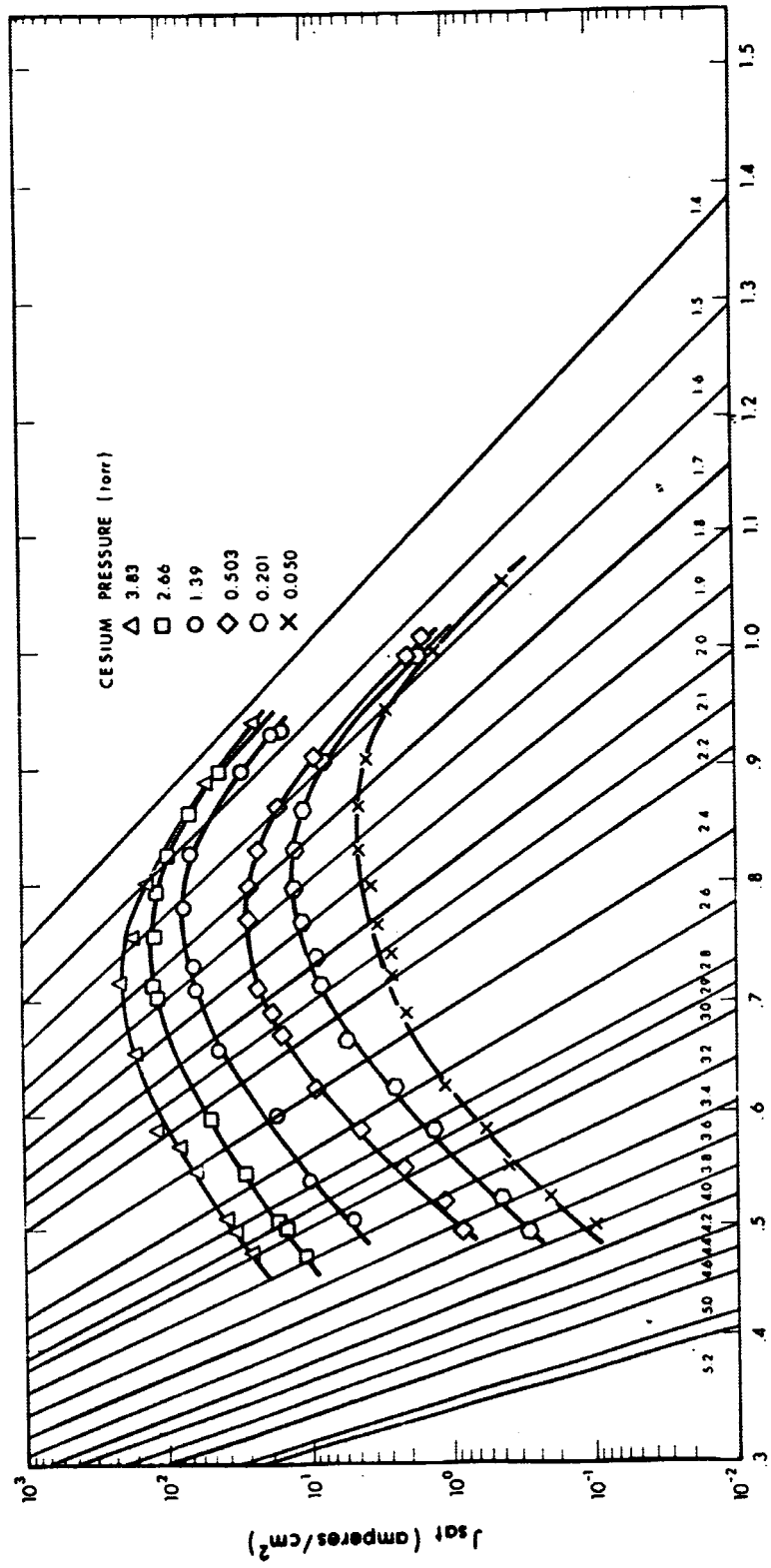

Figure 4. Langmuir "S" Curves for Cesiated Polycrystalline Rhenium Electrodes

is defined as the intersection of the extrapolated Schottky slope and the slope of the ignited region. The interelectrode spacing was set at approximately 4 mils for the curves at pressures of 0.50, 0.20 and 0.05 torr, and at 5 mils for the curves at pressures of 3.83, 2.66, and 1.39 torr. In EOS Report 4006-M-3, a set of Langmuir "S" curves was presented where all emitter temperatures were given as true hohlraum temperatures between 1400°K and 2000°K. Below 1400°K the emitter temperature was determined by platinum, platinum -10% rhodium thermocouples. The thermocouples were calibrated by micro-optical pyrometer determinations in the range where the two overlap. The thermocouples were attached to the emitter by tantalum pads at the same distance from the emitting surface as the hohlraum. Since precise determination of the work function requires knowledge of the emitting surface temperature, a computer program was undertaken to calculate the surface temperature for every data point on the Langmuir "S" curves presented in EOS Report 4006-M-3. The following quantities were taken into consideration in determining the heat balance of the device:

1. $Q_{Rad} = \epsilon \sigma (T_E^4 - T_c^4) A_E$ (1)

   ϵ = effective emissivity

   σ = Stephen Boltzmann constant

   A_E = emitting area

2. Electron Cooling

   $Q_{ec} = \dot{i} (\phi_E + V_m + \frac{2kT_E}{e})$ (2)

   $\dot{i}$ = drift current

   ϕ_E = emitter work function (3)

   $V_m = \frac{k_{TE}}{e} \ell n \frac{\dot{i}sat}{\dot{i}}$

3. Emitter Envelope Heat Losses

$$Q_{en} = \frac{k_{en}\,(T_E - T_c)}{\left(\frac{L}{A}\right)_{en}} - \frac{1}{2}\, i^2\, \rho_{en} \left(\frac{L}{A}\right) \qquad (4)$$

k_{en} = thermal conductivity of envelope material

$\left(\frac{L}{A}\right)_{en}$ = 15 cm^{-1} for the envelope

ρ_{en} = electrical resistivity of envelope material

4. Cesium Conduction Losses (From Experimental Data)

The total heat lost from the emitter is then,

$$Q_T = Q_{Rad} + Q_{ec} + Q_{en} + Q_{cs} \qquad (5)$$

and with this, the electrode surface temperature can be determined from the following equation.

$$T_{E.s.} = T_{E.h.} - \frac{Q_T}{k_E} \left(\frac{L}{A}\right)_E \qquad (6)$$

$T_{E.s.}$ = emitter surface temperature

$T_{E.h.}$ = true hohlraum temperature

k_E = thermal conductivity of emitter material

$\left(\frac{L}{A}\right)_E$ = (0.0456) cm^{-1} for emitter

The polycrystalline rhenium electrode vehicle was operated for approximately 1100 hours during JPL Contract 951225. On the present program the vehicle has received an additional 580 hours on test for a total of 1680 hours. The present testing was terminated when it was found that saturated emission at high cesium pressures (above 2.66 torr) did not correspond to earlier data. Saturated emission values corresponding to the lower pressures on the Langmuir "S" curve were obtained, but raising the cesium reservoir temperature did not produce a

corresponding increase in saturated emission. Figure 5a is an I-V sweep produced at an emitter temperature of 1651°K, and a pressure of 0.503 torr. The saturated emission is found to be 6.5 amps/cm^2, which is in good agreement with Figure 4. Figure 5b is an I-V sweep produced at an emitter temperature of 1651°K, and a cesium reservoir temperature of 316°C. The saturated emission from Figure 5b is 30 amps/cm^2, (corresponding to about 2 torr) which is approximately 30 amps/cm^2 lower than the value at 2.73 torr found in Figure 4. After approximately 100 hours, it was found that the saturated current at 1651°K regardless of the reservoir temperature had dropped to 10 amps/cm^2 corresponding to a pressure of 0.9 torr. At pressures below which normal saturated current could be achieved, it was noted that the voltage output did not degenerate. The test system was vented to air three separate times with a subsequent saturated emission check after each venting. It was found that the emission did not decrease as a step function with venting, but rather continued to decrease as a function of operating time only. It was thus concluded that the system most likely did not have a leak, but was depleted of cesium.

2.2 POLYCRYSTALLINE MOLYBDENUM

A 99.98% pure polycrystalline molybdenum sample was cut from an arc-cast plate purchased from Climax Molybdenum and electron beam welded into a molybdenum support structure for emission measurements in the vacuum emission vehicle and in the thermionic emission microscope. The objective of the measurements was twofold. The first endeavor was to make a precise comparison of effective work functions determined by the two instruments. This was accomplished in the following manner: First, the emission from each grain of the sample was measured in the thermionic emission microscope by taking an average of at least three readings from different areas on the same grain. After all the grains were examined, the sample was removed from the microscope and a photomicrograph of the sample was taken and enlarged to a magnification of

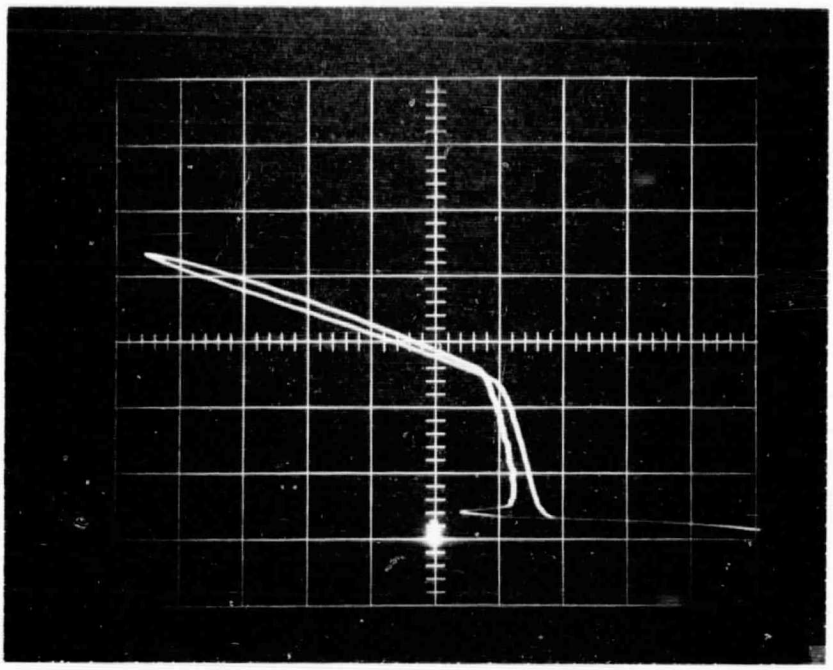

Figure 5a. T_E = 1651°K, P_{cs} = 0.503 torr, 5 amperes/ .2 volts. Collector saturated emission = 6.5 $\frac{\text{amps}}{\text{cm}^2}$

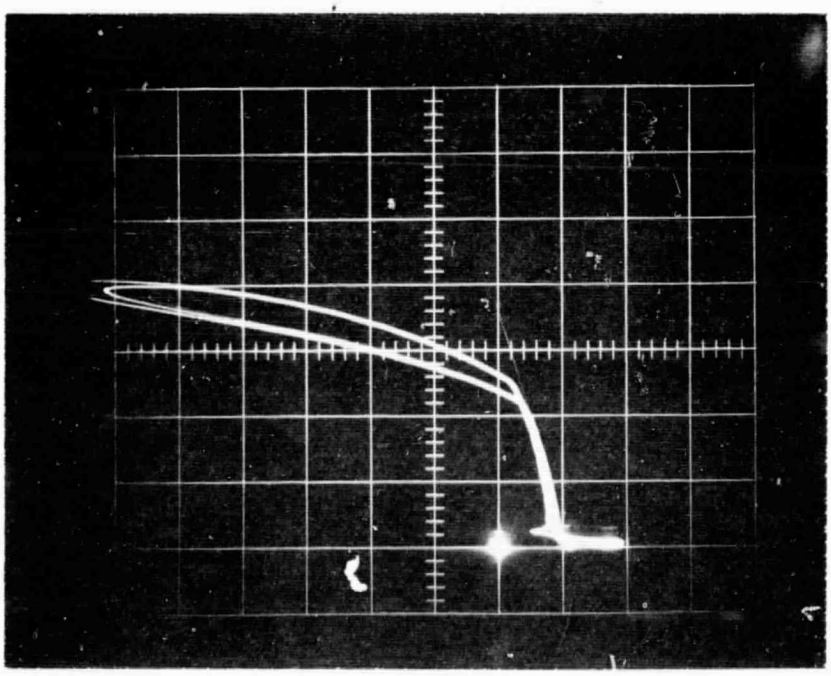

Figure 5b. T_E = 1651°K, P_{cs} = 2.73 torr, 20 amperes/ .2 volts. Collector saturated emission = 30 $\frac{\text{amps}}{\text{cm}^2}$

Figure 5. Saturated Emission Measured from Collector Surface

005338

20X (a photomicrograph was also taken before the sample was put into the microscope so that identification of the grains could be made with respect to a scribe line for the purpose of determining the areas of each grain).

The sample was then installed in the vacuum emission vehicle and a Schottky plot was obtained at exactly the same true hohlraum temperature so that the measured emission and calculated effective work function could be compared directly with the thermionic emission microscope results. Since the sample diameter is considerably larger than the collector diameter of the vacuum emission vehicle, a special procedure was used to determine the exact sample area contributing to the measured emission. After the measurements were completed the collector was removed, leaving the guard ring and sample in place. Since the clearance between collector and guard ring was only about one mil, with the collector removed, the sample was scribed while still in place, and the precise sample area was measured. A photomicrograph was again taken after removing the sample from the vacuum emission vehicle and enlarged to 20X. Initially, the molybdenum sample was high-fired at 2323°K for 16 hours to grow large grains and to stabilize the structure. Subsequent operation during the microscope and vacuum emission testing did not cause detectable changes in the size of the grains. Since the grains remained the same throughout all testing, as evidenced by comparing the "before and after" photomicrographs, a direct correlation was possible between the two testing methods. The photomicrograph of the sample after being scribed for determination of the exact vacuum emission vehicle collecting area was evaluated with a planimeter to determine the area of each individual grain. With this information in conjunction with the corresponding effective work function, an averaged effective work function was calculated and compared with the average effective work function determined from vacuum emission vehicle measurements.

The second object of the experiment was to provide a correlation between the effective work function of the individual grains as determined with the thermionic emission microscope and the crystallographic orientation of the grains. After completion of the testing mentioned above, the sample was sent out for x-ray determination of the sample grains. Resolution of the Laue Pin-hole back reflection x-ray analysis requires grains of at least a 1-millimeter diameter. Because of this, a number of small grains in the sample are not included in the x-ray analysis. Since the cost would be prohibitive to determine the orientation of all 82 grains over 1-millimeter diameter, the grains exhibiting the highest and the lowest work function and approximately 18 grains in between will be analyzed.

2.2.1 THERMIONIC EMISSION MICROSCOPE

The electron emission microscope was operated at a magnification of approximately 80X to accommodate the relatively large grains of the polycrystalline molybdenum. The effective work functions of the grains were determined by individual Faraday cage measurements. Before mounting in the microscope, the sample surface was fine-polished with Linde alumina A, B, and C, and then high-fired for 16 hours at 2323^{o}K. The sample was then diamond-scribed and secured in the microscope. The performance of the Faraday cage was characterized by varying the decelerating voltage and plotting it as a function of Faraday cage current. The grid voltage was 200V, and the accelerating voltage was 12,250V for the curve generated in Figure 6. It can be seen that in the range of operation of the decelerating grid voltage (i.e., 180 to 220V), the Faraday cage current collected is independent of the decelerating voltage.

The results of the thermionic emission microscope measurements are listed in Table I, along with the calculated effective work functions. All of the grains within the area "viewed" by the vacuum emission

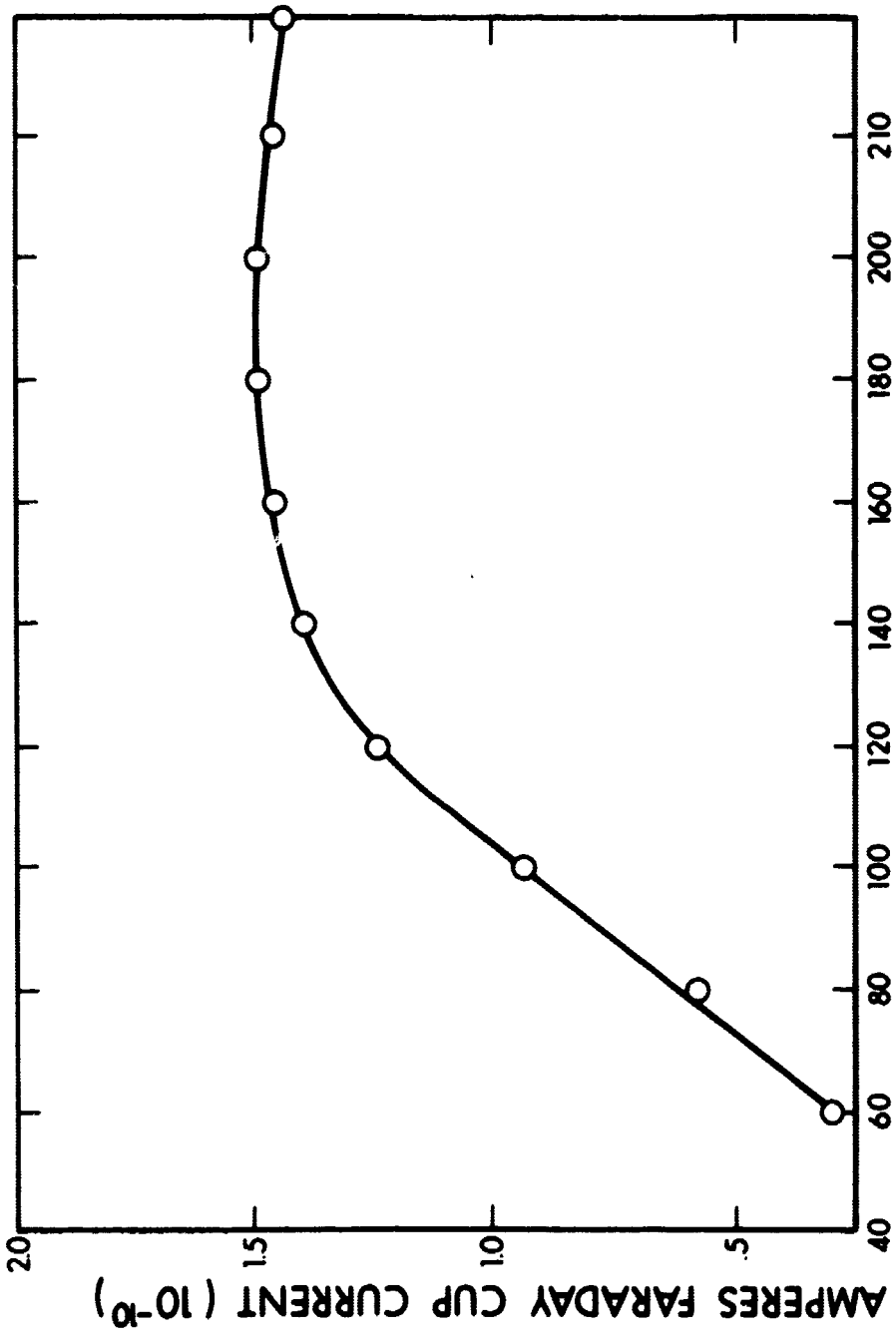

Figure 6. Faraday Cage Current versus Decelerating Voltage

vehicle collector were examined. Those outside this area are listed as such. As already mentioned, the x-ray analysis is confined to grains over 1 mm in diameter, thus the grains were separated into two general categories. Figure 7 is a photomicrograph of the sample area corresponding to the collecting area of the vacuum emission collecting area, showing the numbered grains referred to in Table I.

The averaged effective work function calculated from the microscope/Faraday cage emission measurements of all the grains shown in Figure 7 was determined to be 4.54 e.v. The true hohlraum temperature of the sample was kept exactly at 1789°K for all measurements and was checked before and after every determination. The magnification was checked for each measurement.

The sample electron current density and the Faraday cage current can be related by the equation:

$$J_o = \frac{I \cdot M^2}{A_c}$$

where I is the current from the sample as measured in the Faraday cage, M is the magnification of the microscope, A_c is the area of the collecting hole in the center of the screen, and J_o is the emitter current density.

2.2.2 VACUUM EMISSION VEHICLE

Upon completion of the thermionic emission microscope measurements, the polycrystalline molybdenum sample was removed from the microscope and mounted in the vacuum emission station. The electron gun was set in place with respect to the back of the sample surface and was not disturbed in transit from one measurement system to the other.

TABLE I

EFFECTIVE WORK FUNCTION OF POLYCRYSTALLINE MOLYBDENUM DETERMINED FROM THERMIONIC EMISSION MICROSCOPE FARADAY CAGE MEASUREMENTS AND CORRESPONDING PLANIMETER DETERMINATIONS OF GRAIN AREAS

Grain Over 1 mm Diameter	J_o $\frac{amps}{cm^2}$	ϕEff	Magnification	Area cm^2
1	1.16	4.417	82X	0.021813
2	0.520	4.569	82X	0.023675
3.	0.542	4.563	82X	0.010374
4	0.955	4.478	82X	0.035113
5	0.540	4.564	82X	0.022345
6	1.08	4.463	82X	0.11944
7	0.664	4.704	82X	0.021281
8	0.532	4.565	82X	0.046552
9	0.484	4.605	82X	0.015162
10	0.437	4.617	82X	0.009044
11	0.658	4.533	82X	0.034581
12	0.633	4.540	82X	0.022079
13	0.470	4.609	83X	0.016492
14	0.753	4.511	83X	0.01729
15	0.734	4.515	83X	0.0093104
16	0.465	4.610	83X	0.012236
17	0.423	4.621	83X	0.02952
18	0.610	4.545	83X	0.018886
19	1.49	4.428	83X	0.01596
20	0.470	4.609	83X	0.013832
21	0.397	4.650	83X	0.00532
22	0.639	4.538	83X	out of collector area
23	0.904	4.483	83X	0.00665
24	1.12	4.460	83X	out of collector area
25	0.971	4.476	83X	0.00372

TABLE I

EFFECTIVE WORK FUNCTION OF POLYCRYSTALLINE MOLYBDENUM DETERMINED FROM THERMIONIC EMISSION MICROSCOPE FARADAY CAGE MEASUREMENTS AND CORRESPONDING PLANIMETER DETERMINATIONS OF GRAIN AREAS (contd)

Grain Over 1 mm Diameter	J_o $\frac{amps}{cm^2}$	ϕEff	Magnification	Area cm^2
26	0.538	4.564	83X	0.02952
27	0.406	4.626	83X	0.02713
28	1.42	4.433	83X	0.01463
29	0.388	4.630	83X	0.04602
30	0.576	4.554	83X	0.05879
31	0.412	4.624	83X	0.06730
32	0.834	4.496	83X	0.01543
33	2.34	4.354	83X	0.00665
34	1.45	4.431	83X	0.06251
35	0.473	4.608	83X	0.01649
36	0.454	4.613	83X	0.04735
37	0.423	4.6211	83X	0.01091
38	1.913	4.418	83X	0.01649
39	0.437	4.617	83X	0.004788
40	1.74	4.406	83X	0.05580
41	1.57	4.421	83X	0.01676
42	0.630	4.540	83X	0.004789
43	0.738	4.516	83X	out of collector area
44	0.529	4.567	83X	0.01995
45	1.95	4.388	83X	0.01144
46	1.62	4.417	83X	0.05480
47	1.99	4.385	83X	0.03272
48	1.23	4.450	83X	0.02953
49	0.507	4.572	83X	0.01835
50	0.462	4.610	83X	0.5081
51	0.538	4.564	83X	0.02713
52	0.442	4.616	83X	0.01117

TABLE I

EFFECTIVE WORK FUNCTION OF POLYCRYSTALLINE MOLYBDENUM DETERMINED FROM THERMIONIC EMISSION MICROSCOPE FARADAY CAGE MEASUREMENTS AND CORRESPONDING PLANIMETER DETERMINATIONS OF GRAIN AREAS (contd)

Grain Over 1 mm Diameter	J_o $\frac{amps}{cm^2}$	ØEff	Magnification	Area cm^2
53	0.784	4.505	83X	0.00585
54	0.445	4.645	83X	out of collector area
55	1.01	4.469	83X	out of collector area
56	1.77	4.404	83X	0.01330
57	1.74	4.406	83X	0.03910
58	0.450	4.614	83X	0.02048
59	1.30	4.444	83X	0.01064
60	1.64	4.415	83X	0.03405
61	0.879	4.487	83X	0.01170
62	0.445	4.615	83X	0.01623
63	0.563	4.558	83X	0.01596
64	1.647	4.414	82X	0.02048
65	0.566	4.557	82X	0.01064
66	0.776	4.507	82X	0.00745
67	0.661	4.532	82X	0.0085
68	0.487	4.604	82X	0.01250
69	1.274	4.447	82X	0.01729
70	0.971	4.476	82X	0.01995
71	1.677	4.411	82X	0.02341
72	0.728	4.517	82X	0.00958
73	0.902	4.483	82X	0.01410
74	0.476	4.608	82X	0.01037
75	0.450	4.614	82X	0.01862
76	0.795	4.503	82X	out of collector area
77	0.635	4.539	82X	out of collector area
78	0.551	4.561	82X	out of collector area

TABLE I

EFFECTIVE WORK FUNCTION OF POLYCRYSTALLINE MOLYBDENUM DETERMINED FROM THERMIONIC EMISSION MICROSCOPE FARADAY CAGE MEASUREMENTS AND CORRESPONDING PLANIMETER DETERMINATIONS OF GRAIN AREAS (contd)

Grain Over 1 mm Diameter	J_o $\frac{amps}{cm^2}$	ØEff	Magnification	Area cm^2
79	0.506	4.673	82X	0.01809
80	0.941	4.479	82X	out of collector area
81	1.42	4.434	82X	out of collector area
82	0.355	4.639	82X	0.01277
Grain Under 1 mm Diameter				
1	1.59	4.419	82X	0.00133 0.00159
2	1.59	4.419	82X	0.00266
3	0.697	4.523	82X	0.00452
4	0.353	4.639	82X	0.00452
5	0.672	4.529	82X	0.00346
6	0.706	4.521	82X	0.00239
7	1.41	4.435	82X	0.00186
8	0.571	4.555	82X	0.000798
9	0.520	4.569	82X	0.003192
10	0.580	4.553	82X	0.00319
11	1.64	4.415	82X	0.00133
12	0.731	4.516	82X	0.004788
13	0.882	4.501	82X	0.004788
14	0.790	4.505	82X	0.004256
15	0.588	4.551	82X	0.005586
16	1.76	4.405	82X	0.005586
17	1.21	4.452	82X	out of collector area
18	1.51	4.426	82X	out of collector area
19	0.496	4.602	82X	out of collector area
20	0.546	4.562	82X	0.00372

TABLE I

EFFECTIVE WORK FUNCTION OF POLYCRYSTALLINE MOLYBDENUM DETERMINED FROM THERMIONIC EMISSION MICROSCOPE FARADAY CAGE MEASUREMENTS AND CORRESPONDING PLANIMETER DETERMINATIONS OF GRAIN AREAS (contd)

Grain Under 1 mm Diameter	J_o $\frac{amps}{cm^2}$	ϕEff	Magnification	Area cm^2
21	0.504	4.573	82X	0.002926
22	0.471	4.609	82X	out of collector area
23	0.799	4.503	82X	out of collector area
24	0.874	4.488	82X	out of collector area
25	0.496	4.602	82X	0.001596
26	0.597	4.549	82X	0.006916
27	0.462	4.611	82X	0.00399
28	0.521	4.569	82X	0.004256
29	0.672	4.529	82X	0.00133
30	1.72	4.408	82X	0.0125
31	0.756	4.511	82X	0.003724
32	0.462	4.602	82X	0.000798
33	0.378	4.633	82X	out of collector area
34	0.563	4.714	82X	0.002128
35	1.22	4.451	82X	0.00665
36	1.82	4.400	82X	0.00505
37	0.748	4.428	82X	out of collector area
38	0.454	4.613	82X	out of collector area
39	1.22	4.451	82X	out of collector area
40	0.756	4.511	82X	out of collector area
41	0.546	4.562	82X	out of collector area
42	2.00	4.384	82X	out of collector area
43	1.81	4.400	82X	0.00984
44	1.73	4.407	82X	0.000532
45	1.60	4.418	82X	0.001064
46	0.773	4.508	82X	0.00452
47	0.697	4.523	82X	0.00745

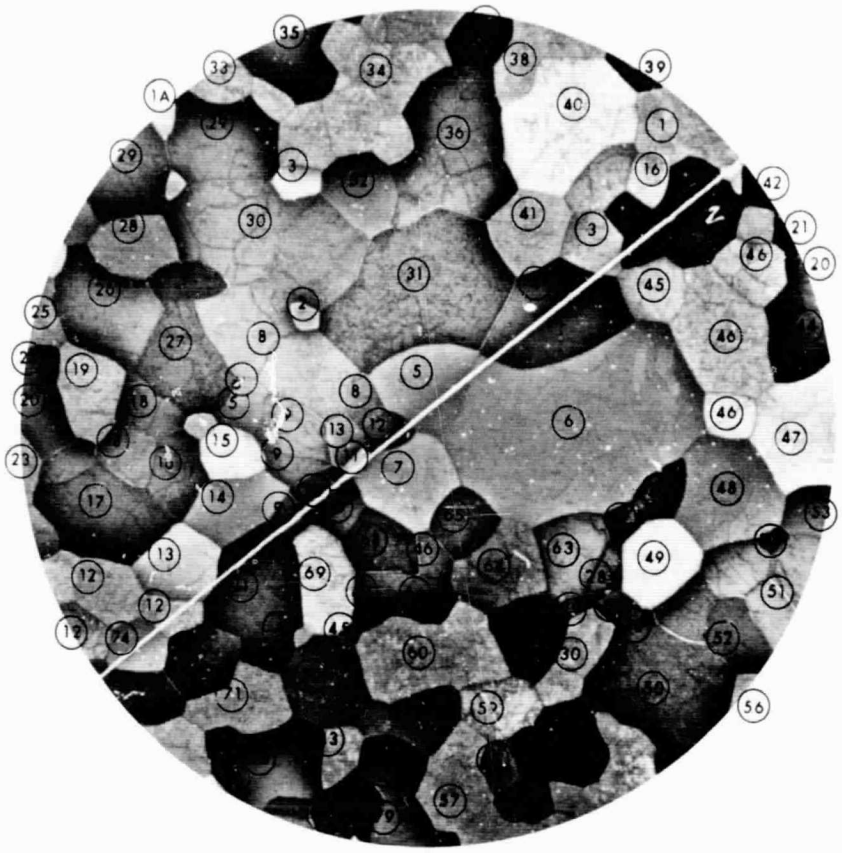

Figure 7. Photomicrograph of Polycrystalline Molybdenum Area Corresponding to Collecting Area of the Vacuum Emission Vehicle. Circled Numbers Refer to Grains Over One Millimeter Diameter. Magnification 7.53X.

Figure 8 is a Schottky plot of the polycrystalline molybdenum sample at a true hohlraum temperature of 1789°K, exactly the same temperature at which the sample was operated in the thermionic emission microscope. The experiment was repeated three times with no significant difference noted between runs. The extrapolated Schottky slope produced an effective work function of 4.48 e.v. This compares within experimental error (±0.04 e.v.) of the value of 4.54 e.v. determined with the thermionic emission microscope of exactly the same area of the button as viewed by the vacuum emission vehicle collector. The theoretical Schottky slope was calculated from the Schottky equation:

$$\text{Log } J_{RS} = \log J_R + (1.912/T)\sqrt{E}$$

where J_R is the zero field Richardson current, and J_{RS} is the Schottky current. The agreement between the experimental and theoretical slopes is reasonable at this low temperature.

Figures 9, 10, and 11 are Schottky plots produced at various temperatures, with the results listed in Table II.

TABLE II

EFFECTIVE WORK FUNCTION OF POLYCRYSTALLINE MOLYBDENUM BY EOS VACUUM EMISSION VEHICLE

T_E °K	Jo amps/cm^2	ϕ e.v.*
1973	1.53×10^{-3}	4.52
1873	3.66×10^{-4}	4.49
1823	1.69×10^{-4}	4.50
1789	9.046×10^{-5}	4.48

* Experimental error ±0.04 e.v.

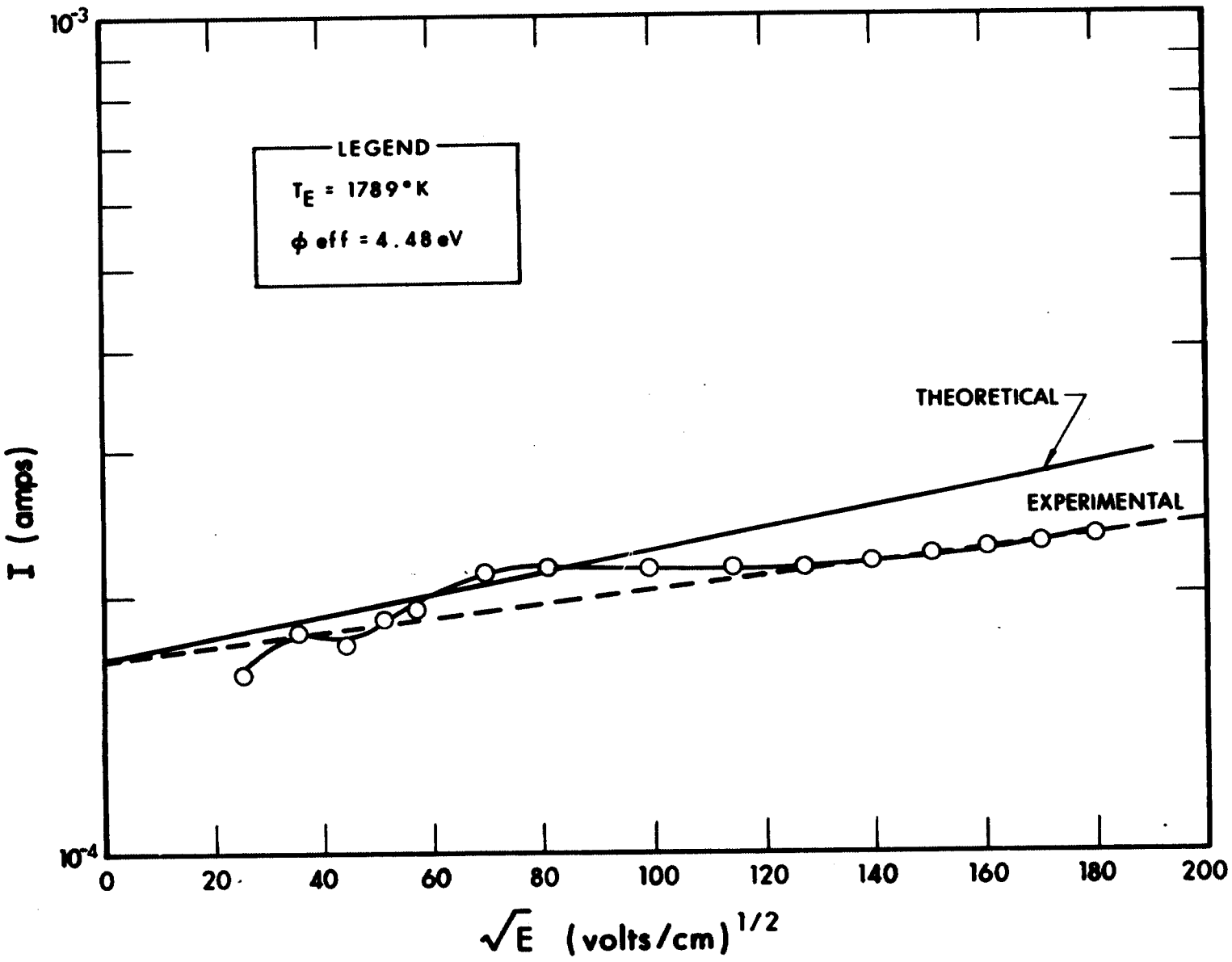

Figure 8. Schottky Plot of Polycrystalline Molybdenum at 1789°K True Hohlraum Temperature as Determined From Vacuum Emission Vehicle Measurements. The Sample was Vacuum Fired at 2323°K for 16 Hours Prior to the Measurement.

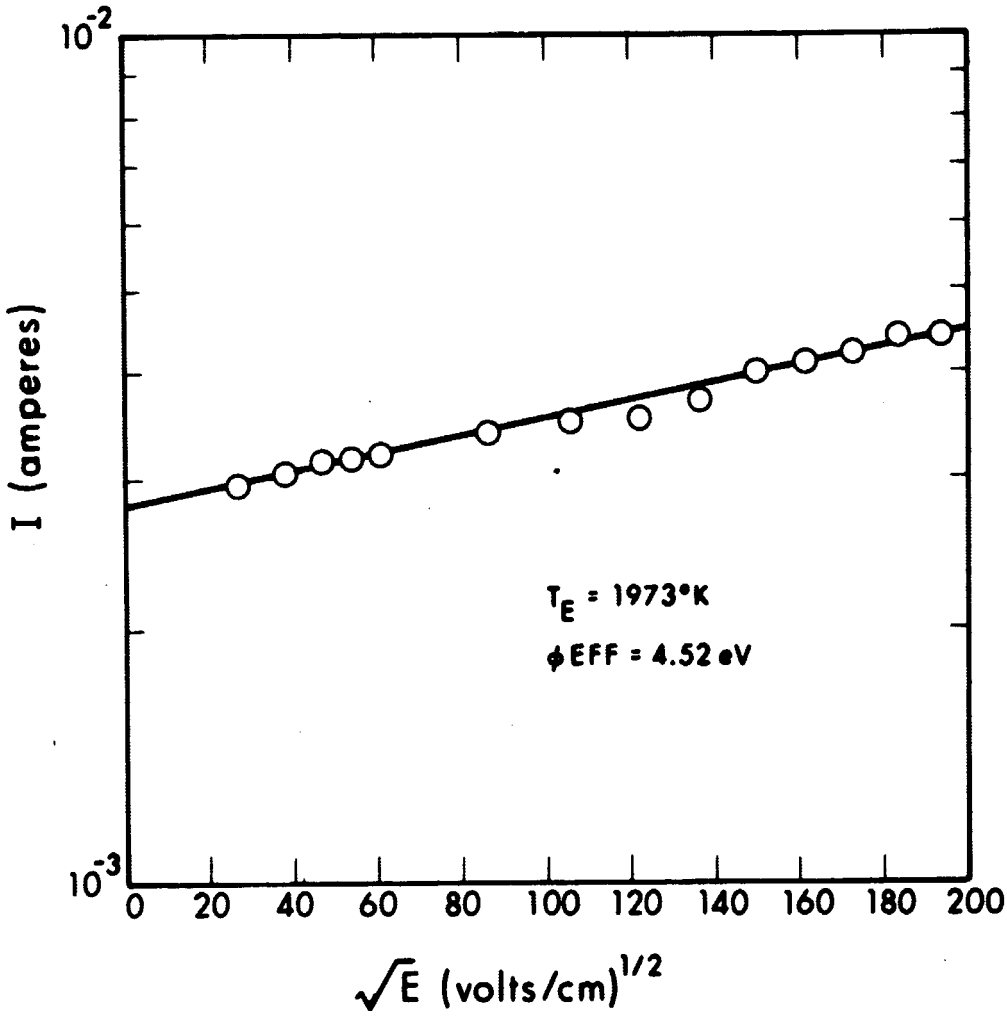

Figure 9. Schottky Plot of Polycrystalline Molybdenum After Vacuum Firing at 2323°K for 16 Hours

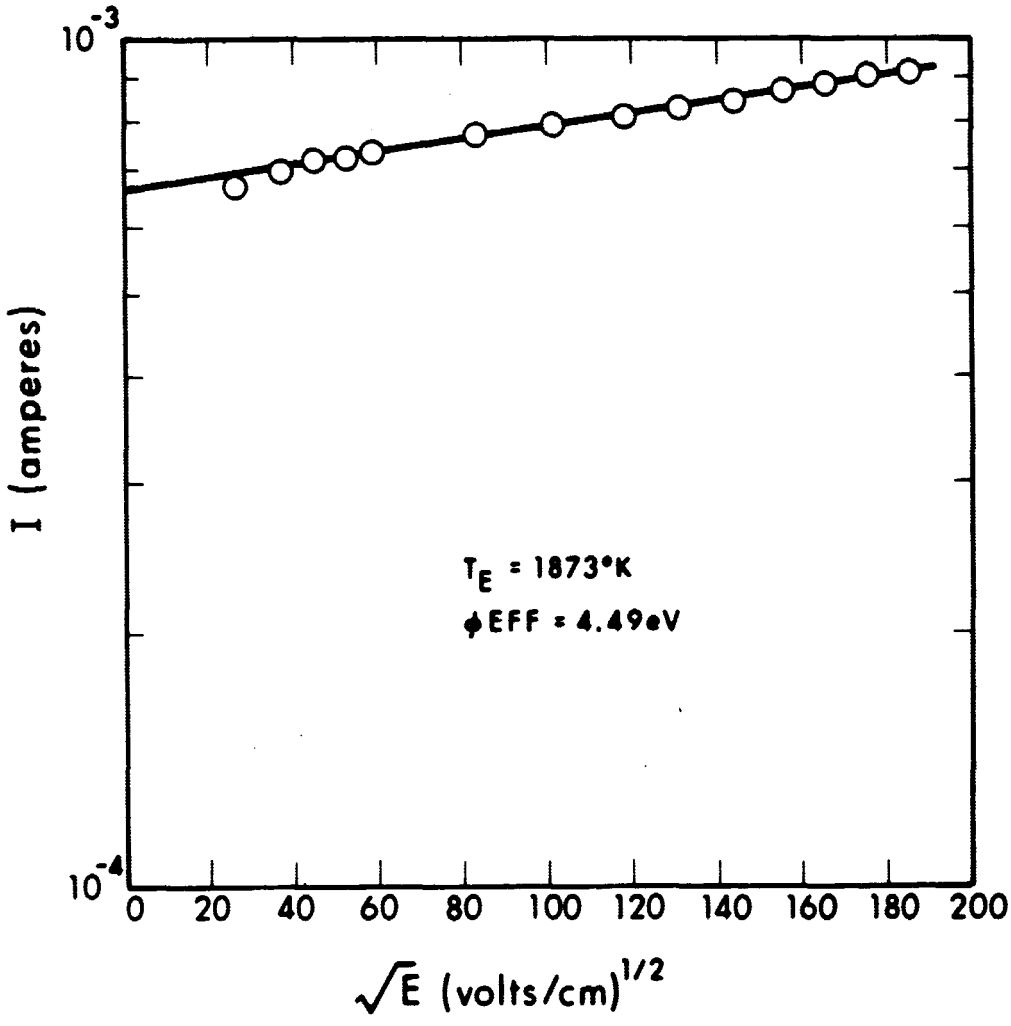

Figure 10. Schottky Plot of Polycrystalline Molybdenum After Vacuum Firing at 2323°K for 16 Hours

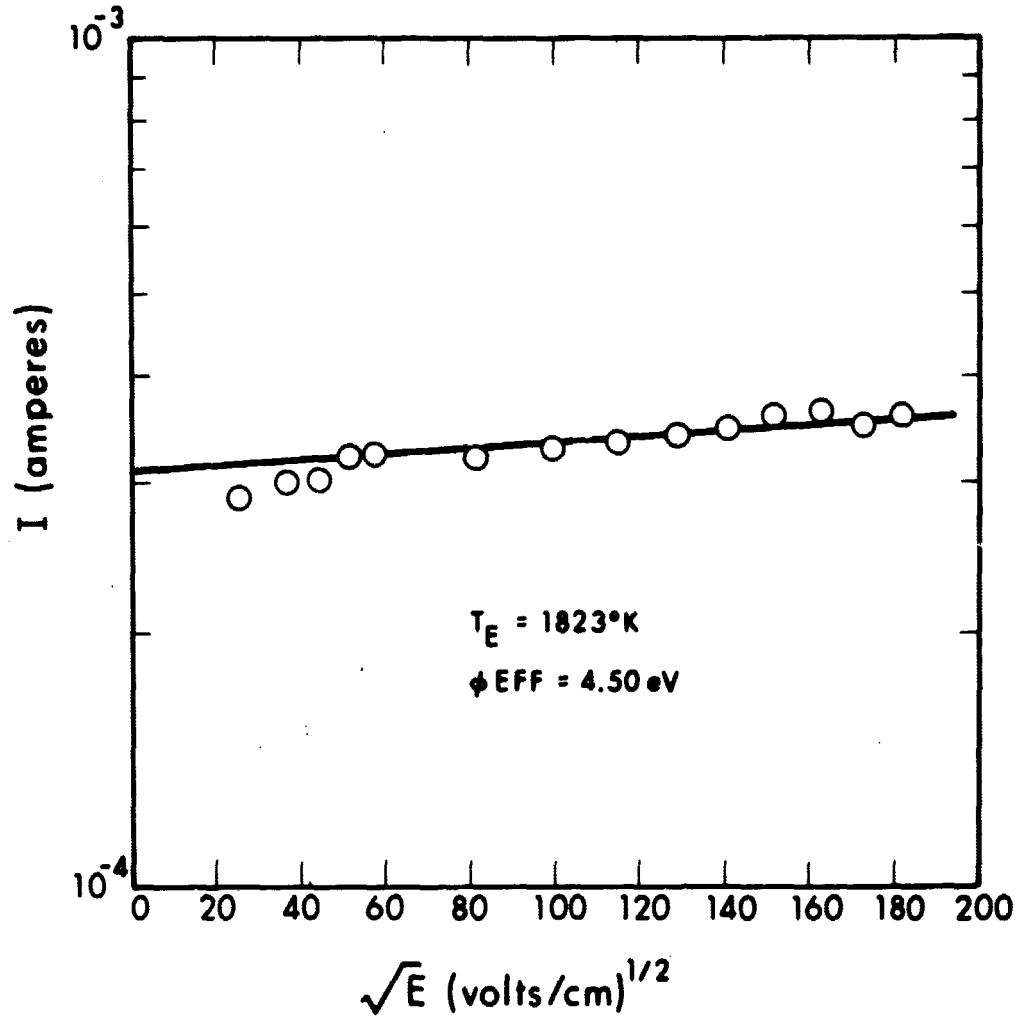

Figure 11. Schottky Plot of Polycrystalline Molybdenum After Vacuum Firing at 2323°K for 16 Hours

SECTION 3

ELECTRODE MATERIALS INVESTIGATION (TASK II)

Six vapor-deposited 22 to 26 percent rhenium/tungsten on 25 percent rhenium/tungsten substrates have had hohlraums spark eroded, finish machined, and vacuum outgassed at 2523°K for one hour. Vapor deposited 22 to 26 percent rhenium/tungsten envelopes for test support structures and for the variable parameter test vehicle and planar converter have been machined and are being brazed onto molybdenum support structures. Since previous EOS variable parameter vehicles and planar converters[1][2] have been fabricated with pure rhenium emitters and envelopes (Figures 12, 13, 14, 15), minor design changes will be required for the present 25 percent rhenium/75 percent tungsten electrode-envelope devices. The heat choke length of the variable parameter vehicle will be lengthened since the thermal conductivity[3] at 1500°K for example is 0.659 watts/cm°K for 25 percent rhenium/75 percent tungsten as compared to 0.50 watts/cm°K for pure rhenium. The electrical resistivity[3] of 25 rhenium/75 tungsten is 57.4 μohm-cm at 1000°C as compared to approximately 80 μohm-cm for pure rhenium. The planar converter spacing determination will require further calculations also with the thermal coefficient of expansion[4] of 25 rhenium/75 tungsten given as

$$\frac{L - L_{25^\circ C}}{L_{25^\circ C}} \times 100 = A + BT + CT^2,$$

where expansions are referred to the length at 25°C. The temperature, T, is in °C, and the constants are:

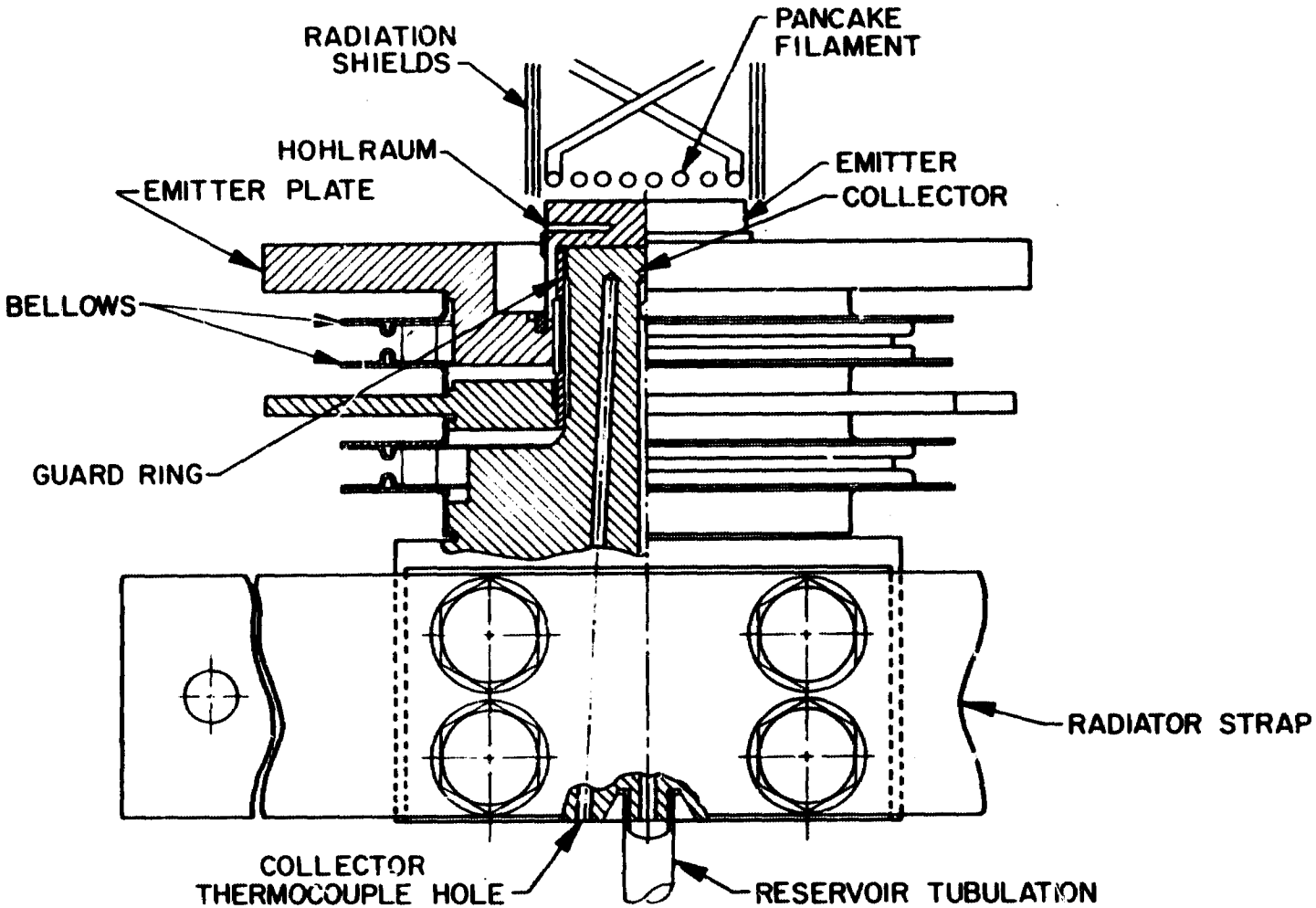

Figure 12. Variable Parameter Test Vehicle Basic Design.

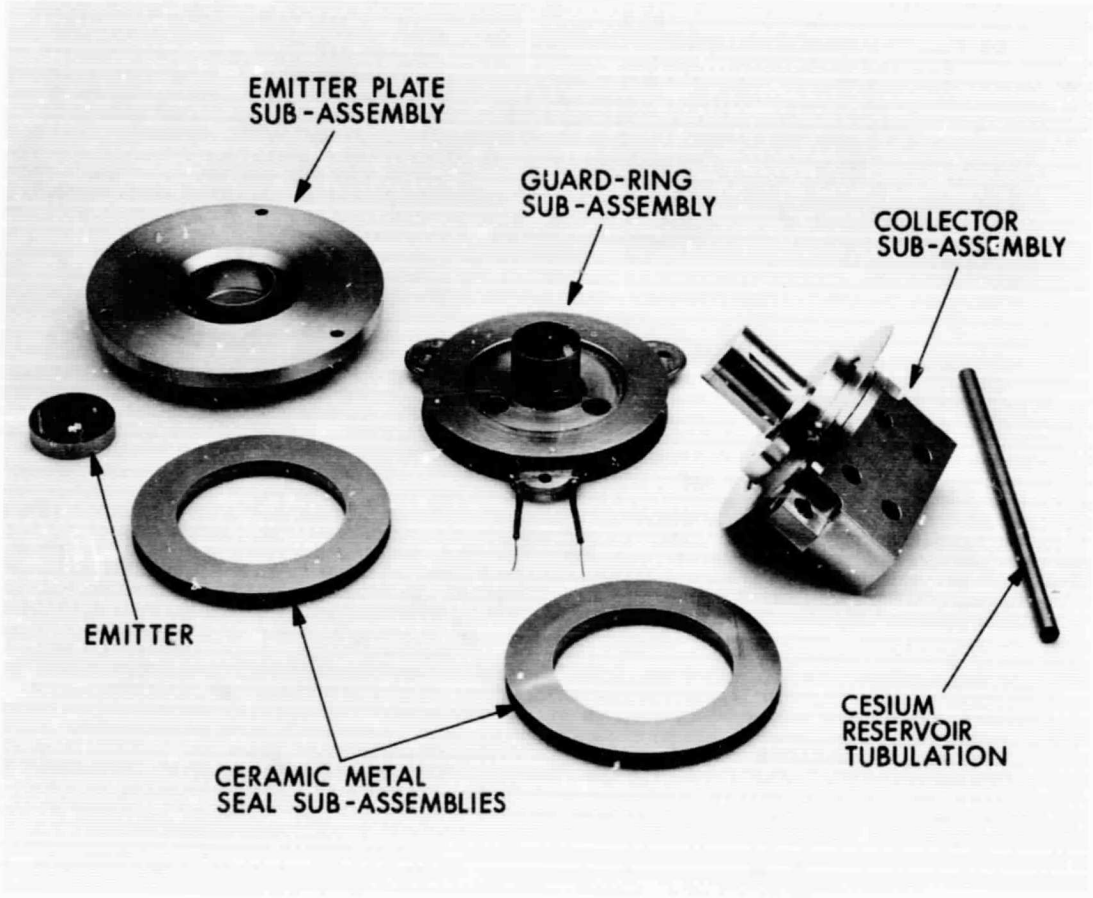

Figure 13. Variable Parameter Test Vehicle Subassemblies and Components

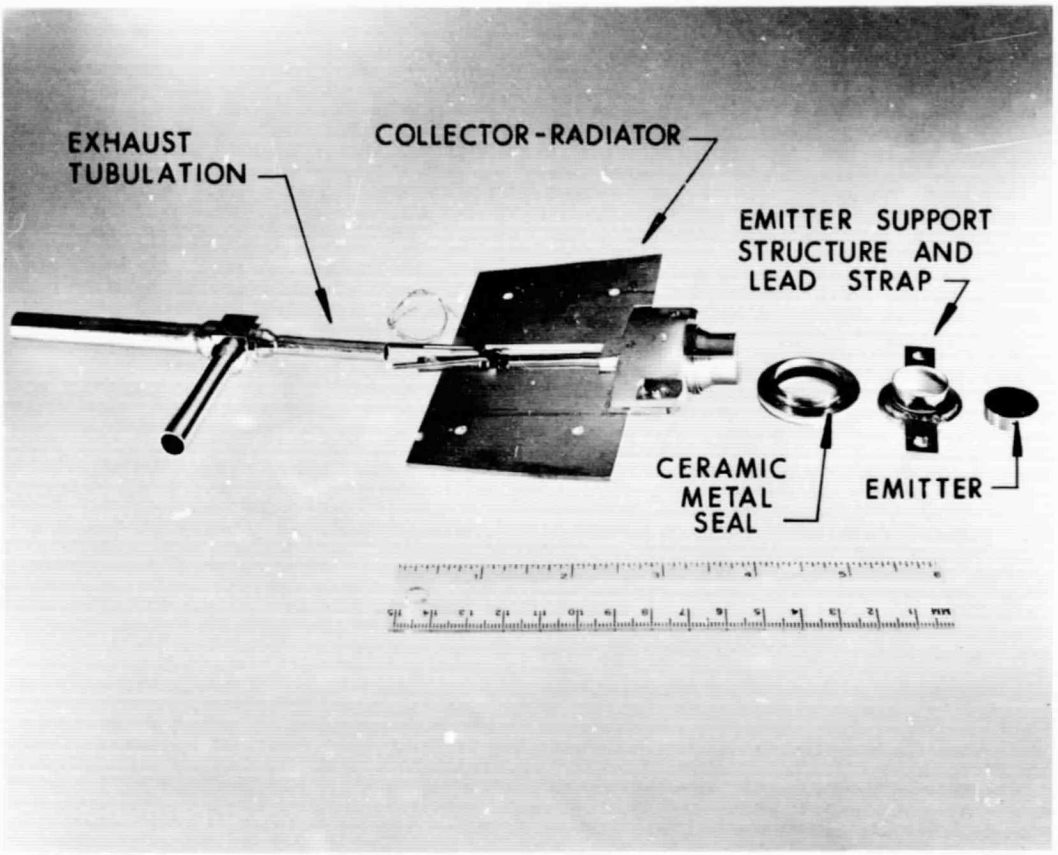

Figure 14. Layout of Principal Subassemblies of EOS High-Performance Planar Thermionic Converters

566132

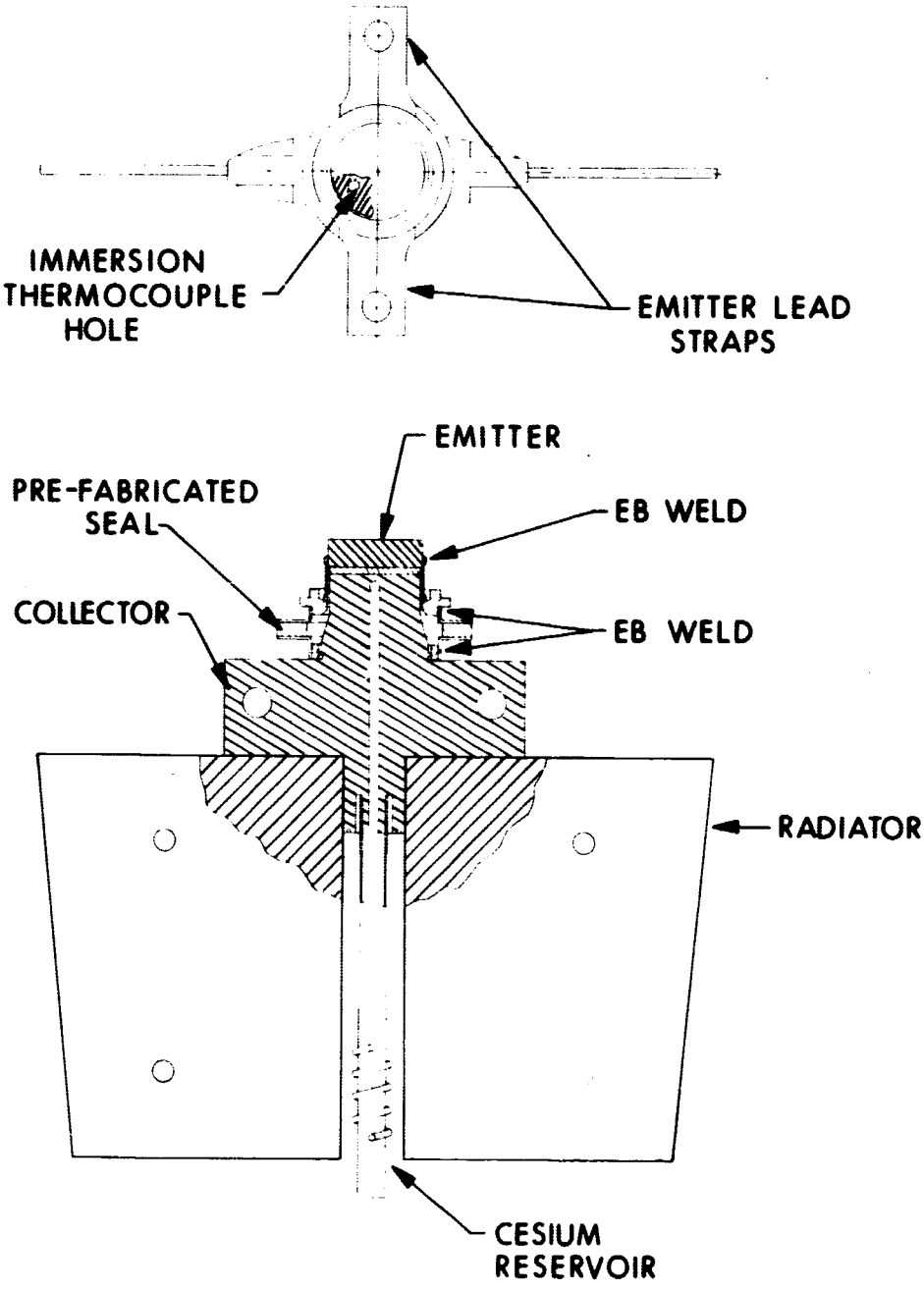

Figure 15. Completed Planar Diode Assembly

$$A_o = -8.46 \times 10^{-4}$$

$$B_4 = 3.91 \times 10^{-4}$$

$$C = 1.14 \times 10^{-7}$$

The applicable temperature range for the above equation is 25°C to 2500°C.

Variable parameter test vehicle and planar converter piece parts are nearly completed so that devices can be fabricated upon completion of the electrode property investigations in the vacuum emission vehicle and thermionic emission vehicle.

SECTION 4

LOW TEMPERATURE (1700°K-1800°K) CYLINDRICAL CONVERTER (TASK III)

Four cylindrical converters (SN109CA, SN109CB, SN110CA, and SN110CB) consisting of vapor-deposited rhenium electrodes have been designed and are being fabricated in an iterative manner to provide performance comparison to planar converters of the same electrode material developed under NASA contract NAS7-514. Each converter has an emitter area of 2.0 cm^2 and collecting area of 1.88 cm^2 to provide an exact performance comparison.

The cylindrical converters were designed for maximum performance at the emitter and interelectrode spacings specified below:

Converter designation	Emitter temperature	Design Criteria: Interelectrode spacing	Design Criteria: Power output
SN109CA, SN109CB	1800°K	6^{+1}_{-0} mils	10.5 w/cm^2
SN110CA, SN110CB	1700°K	10^{+1}_{-0} mils	4.5 w/cm^2

4.1 CONVERTER DESIGN

The design of SN109CA has been completed by EOS, reviewed and approved by JPL and reported in detail in the first quarterly report of this contract.

The SN109CA converter assembly is shown in Figure 16. The design incorporates four major subassemblies; the emitter, the emitter support structure (i.e., emitter lead straps and emitter heat choke), the prefabricated seal assemblies, and the collector-radiator. These major subassemblies are electron beam welded together to form the final cylindrical converter configuration.

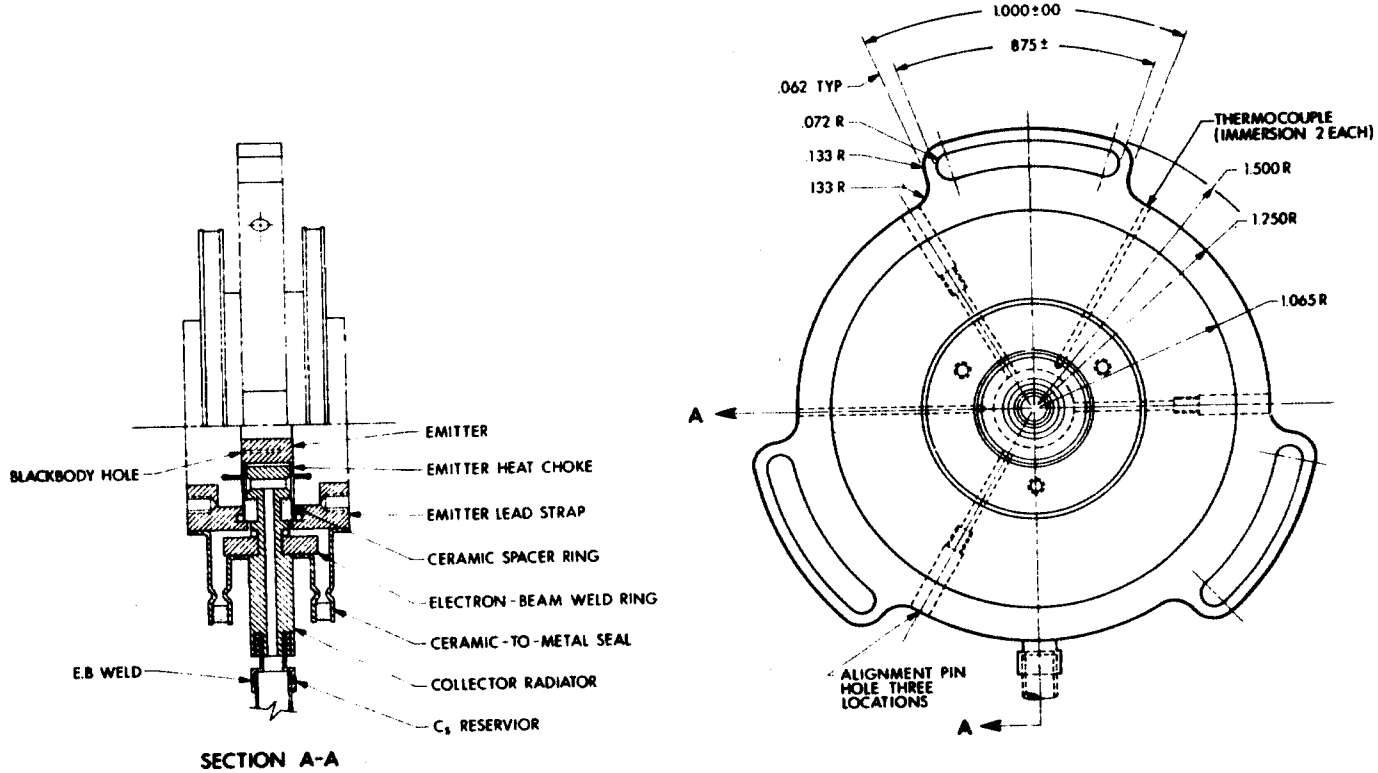

Figure 16. SN109CA Converter Assembly

One problem area peculiar to cylindrical converter geometries is the concentricity of electrodes. Therefore, alignment pins (refer to Figure 16) have been incorporated into this design to establish and retain a 10% concentricity of the electrodes during fabrication. The major subassemblies of the converter are electron beam welded with the alignment pins in place. The pins are then removed and the holes are plugged and electron beam welded shut to form a vacuum-tight diode assembly.

Electron beam welding schedules for the major subassemblies and alignment pin plugs are discussed below.

4.2 RADIATOR HEAT REJECTION

An integral molybdenum collector-radiator with cutouts for the ceramic spacing ring and niobium electron beam welding ring was fabricated to provide a full scale test for radiator heat rejection of the computed collector heat load of 129 watts (Ref. 5). Figure 17 shows the temperature profile of the cutout collector radiator assembly as a function of the collector surface temperature. To ascertain the temperature drop in this structure due to the cutouts, a second integral molybdenum collector-radiator without cutouts was machined, Rokided, and tested for heat rejection.

Both assemblies were tested in the same manner by placing thermocouples at precisely known intervals across the radiating surfaces to provide temperature profiles at nearly equivalent collector temperatures. The collector surface was heated by electron bombardment.

Figure 18 shows temperature profiles of both the cutout and noncut collector-radiator assemblies plotted for direct comparison. The temperature of the collector surface can be seen to be essentially equal for each pair of temperature profiles to be compared (i.e., A with A′, B with B′, etc.)

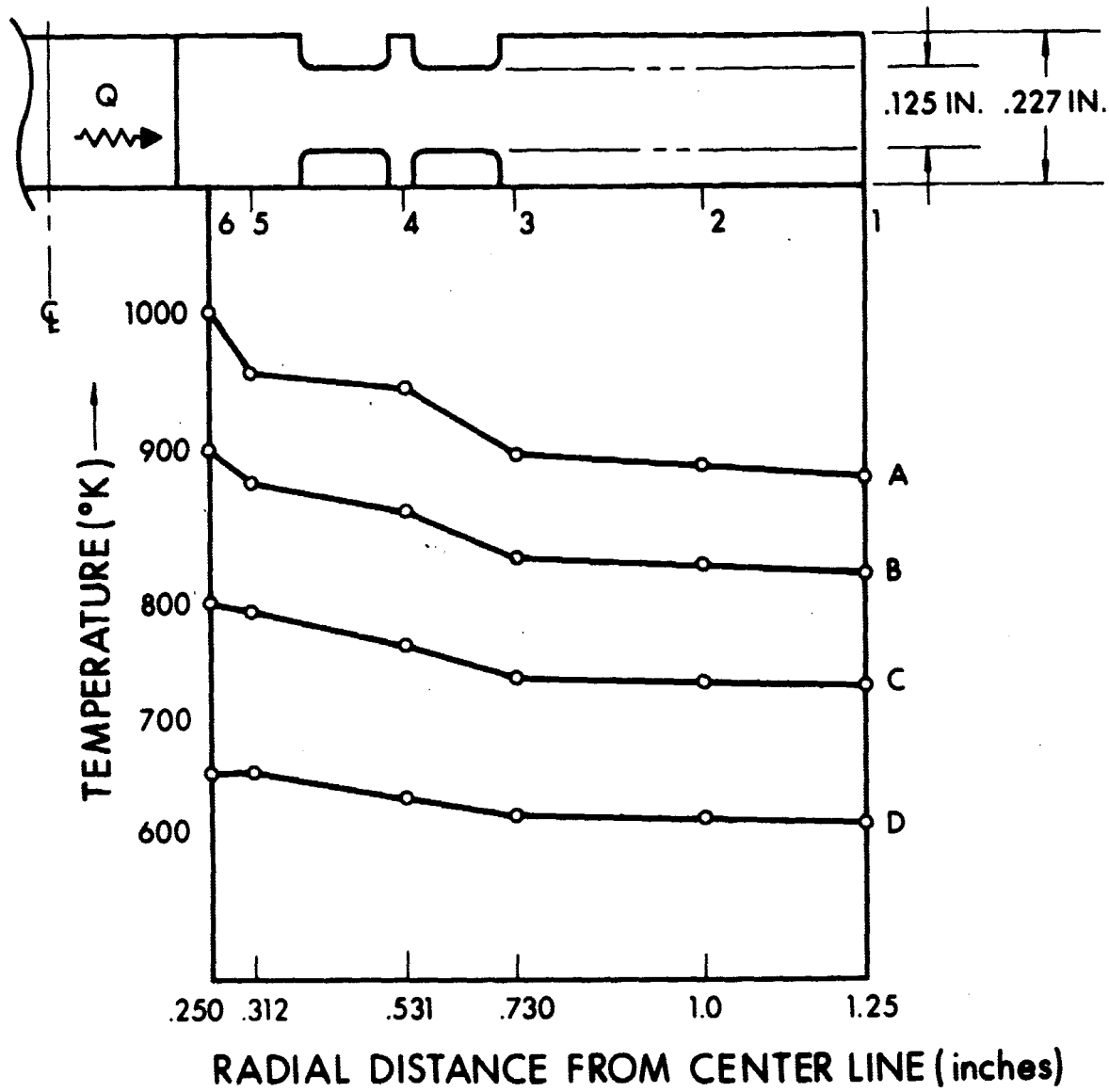

Figure 17. Radial Temperature Distribution of Cutout Collector-Radiator Assembly as a Function of Collector Surface Temperature (same as per SN109CA).

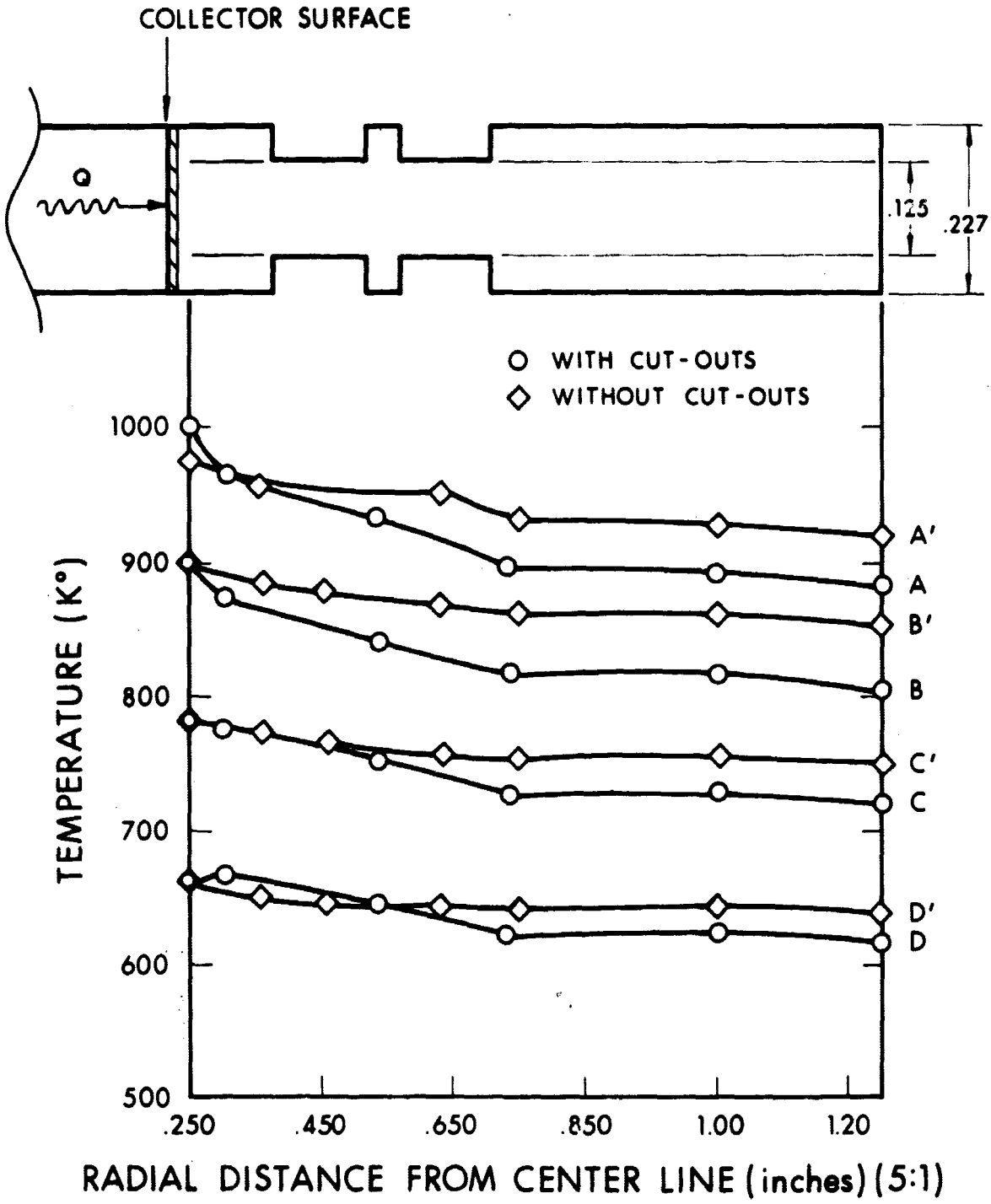

Figure 18. Radial Temperature Distribution Comparing Cutout to Non-cutout Collector-Radiator Assembly, as a Function of Collector Surface Temperature.

Due to the increased thickness of the heat transfer path of the non-cutout collector-radiator assembly, the temperatures at the radiator are higher in each case.

For collector temperatures on the order of 700°C - 800°C, the difference is 25°C of radiator temperature and is not considered a serious penalty.

4.3 MOLYBDENUM/VAPOR-DEPOSITED RHENIUM INTERFACE

The collector radiator subassembly is a molybdenum disc with the central hole vapor-deposited with rhenium. The deposit is applied to the molybdenum substrate before performing any brazing of the welding ring or cesium reservoir adaptor. Some concern arose as to whether the difference in thermal expansion between molybdenum and rhenium would destroy the bond during the brazing process; therefore, two molybdenum cylinders with the central hole vapor-deposited with rhenium were prepared.

The cylinders were separately subjected to 1700°C and 1900°C temperature treatments for 3 minutes to simulate EOS' titanium and vanadium braze schedules, respectively. The specimens were subsequently sectioned and the rhenium-molybdenum bond metallographically examined. A micrograph of the bonded area is shown in Figure 19. This particular specimen shows the formation of a molybdenum-rhenium intermetallic compound -- a result of the titanium braze schedule. The width of the intermetallic zone is approximately 0.0006 inch and the absence of voids or inculsion in the zone qualifies the bond as acceptable for 10,000 hour collector operation. The vanadium schedule produced similar results although the intermetallic zone was two or three times wider. EOS is using titanium and the titanium braze schedule to join the collector subassembly piece parts.

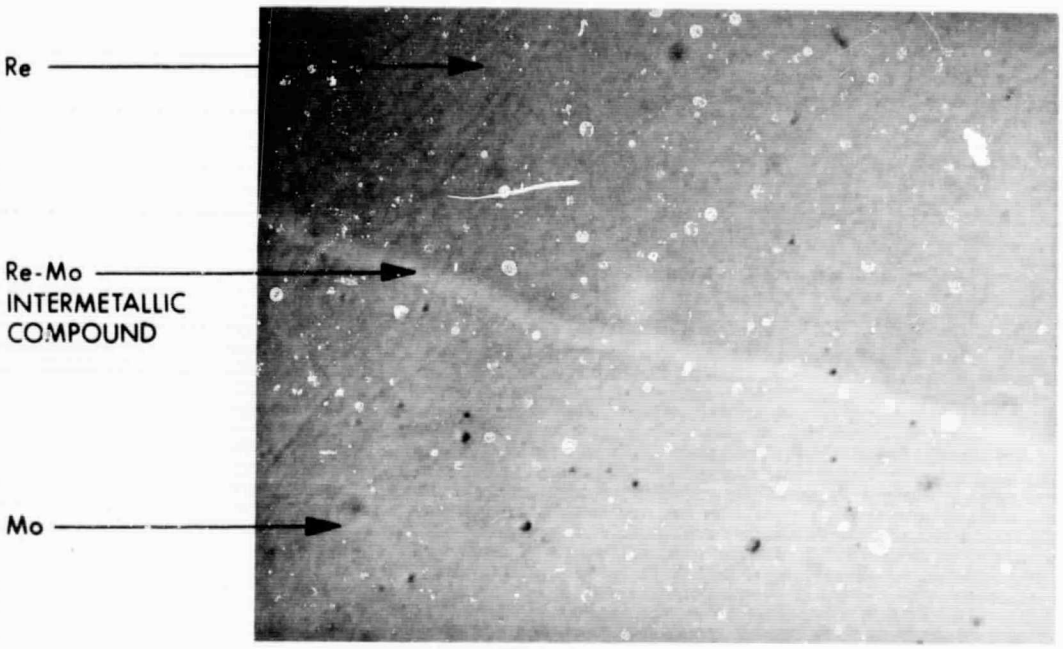

Figure 19. Vapor-deposited Rhenium-Molybdenum Composite that was Subjected to a Titanium Braze Schedule. Microphoto taken at 1500X.

4.4 ELECTRON BEAM WELDING

The choice of vapor-deposited rhenium is an emitter material for a high performance, long life thermionic converter also established rhenium as the emitter support structure (envelope) material. There are two principal reasons supporting this: First, rhenium and the more common structural materials such as tantalum, tungsten, niobium, etc., form low temperature eutectics and brittle intermetallic compounds which lack mechanical strength. Second, even if two such dissimilar materials welded reliably, the emitter becomes "contaminated" with envelope material which diffuses onto the emitter surface. Electron beam welding has proven to be a most effective means of joining converter parts and in particular the emitter-to-emitter support structure. The application of heat is instantaneous, which prevents part warpage; also, the weld zone is small and ductile, which permits thermal cycling without failure.

An experimental investigation was conducted to establish a reliable schedule for electron beam welding vapor-deposited rhenium to rhenium.

An emitter cylinder of vapor-deposited rhenium and two 0.005-in. thick rhenium sheets were machined, chemically cleaned, and spot-welded together to serve as a feasibility sample for two different sets of electron beam welding parameters. Separate welds were made on EOS' Hamilton-Zeiss electron beam welder in a 6×10^{-5} torr vacuum environment. One weld was made with a beam power of 120 KV x 2.0 ma while rotating the sample at 40 rpm. (This weld was leak-tight.) The second weld was made using a higher beam power of 130 KV x 2.0 ma beam power rotating the sample at 40 rpm. (This weld was also leak-tight.)

The weld sample was thermally cycled several times to approximately $1900^{\circ}K$ and again leak checked tight. The sample was prepared metallurgically to examine the penetration achieved by the two welding schedules.

The two beam weld schedules after examination showed that the schedule of 120 KV x 2.0 ma had a beam width of approximately 0.006 in. and a penetration depth of approximately 0.006 in. The 130 KV x 2.0 ma schedule had a beam width of approximately 0.006 in. and a penetration of approximately 0.008 - 0.010 in. deep. It is felt that the latter schedule will yield a reliable, long-life weld.

An investigation was also conducted to determine the feasibility of electron beam welding of molybdenum plugs into the molybdenum collector radiator. The final electron beam weld is made on the cylindrical converter after the alignment pins are removed from the collector radiator subassembly. Molybdenum plugs are inserted into the alignment pin holes and electron beam welded shut. This closure weld must be vacuum-tight and of high integrity.

A successful molybdenum-to-molybdenum weld can be effected as long as certain procedures are followed.

a. The first of these is an extreme cleanliness of joining surfaces and adjacent areas; this involves removing all oxide films. Chemical cleaning baths and vacuum outgassing are reliable methods of guaranteeing the required cleanliness.

b. Secondly, is the need to control the welding atmosphere with respect to oxygen and nitrogen content both of which have a detrimental effect on ductivity of the weld. Vacuum electron beam welding insures minimal gas content.

c. Thirdly, a preheat above $\approx 400^{\circ}C$ of the parts is required to ensure that the molybdenum to be welded is above the ductile-to-brittle transition temperature. The brittle-to-ductile transition temperature in arc cast molybdenum is usually taken to be above $100^{\circ}C$ and upwards to $850^{\circ}C$, depending on purity and previous history.

An arc-cast molybdenum feasibility cylinder was fabricated, chemically cleaned, and vacuum-outgassed at $2000^{\circ}K$. This cylinder was used to simulate the collector-radiator assembly. Arc-cast molybdenum plugs were also fabricated and chemically cleaned.

The feasibility weld was made at a beam power of 110 KV x 5.2 ma after the parts were preheated to approximately 1000°K. The weld was circumferentially made at 40 rpm. The weld was checked leak-tight and cross-sectioned for examination.

Examination revealed the beam penetration was approximately 0.050-in. deep and the beam width was approximately 0.025-in. wide which is considered adequate for reliable closure.

4.5 CYLINDRICAL CONVERTER ASSEMBLY PROCEDURE

The fabrication of the emitter, emitter support structure, ceramic spacers, metal-to-ceramic seals, collector-radiator, and the reservoir subassemblies have been completed for SN109CA. Figure 20 shows these principal subassemblies.

Before the final assembly, the radiator was plasma sprayed with a high emissive coating of Rokide "C". On the first attempt, the coating would not adhere to the molybdenum radiator substrate. Upon close examination, it was found that the substrate had a thin coating of a hard smooth material. It was suspected that the material was a thin layer of rhenium that chemically plated the entire molybdenum structure during the rhenium vapor deposition processing of the collector face. The radiator had to be resurfaced by diamond grinding to remove the surface layer material. The radiator area was abraded to roughen the surface and the coating of Rokide "C" was then successfully applied.

Part of the final assembly operation is the electron beam welding of the prefabricated seal assembly to the collector-radiator niobium weld ring and also to the niobium emitter lead straps. The weld schedule follows parameters established from feasibility experiments that were determined on JPL Contract 951225; that is, an electron beam voltage

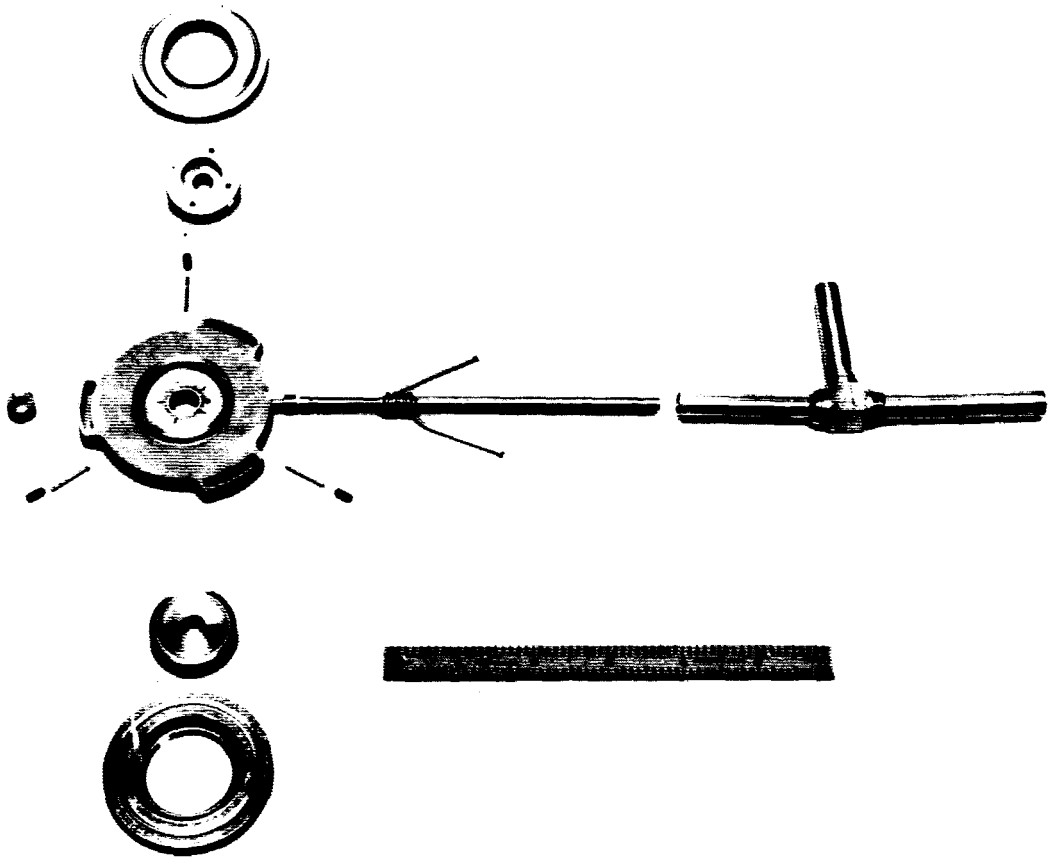

Figure 20. Cylindrical Converter SN109CA Subassemblies

of 150 KV at a current of 2.6 - 2.7 ma with a part revolution of 22 - 25 rpm. Also, electron beam welds are made to join the emitter to the emitter support structure (envelope). The weld schedule is 120 KV x 2.0 ma, as determined by feasibility welds discussed in Subsection 4.4. Attaching the emitter last has one main advantage: It allows for the emitter support structure to be stress-free when making the most critical weld -- that of the emitter. The concentricity of the emitter to the collector during all electron beam welding is retained by the alignment pins. After the flange and emitter welds are made, the alignment pins are removed and the alignment pin channels are closed by electron beam welding molybdenum plugs in the collector-radiator assembly. This schedule is determined also by feasibility welds as discussed in Subsection 4.4 (i.e. 110 KV x 5.2 ma, part rotation of 40 rpm, after parts were preheated to approximately 1000^{o}K).

The exhaust tubulation is joined to the cylindrical converter assembly, the assembly is now ready for final processing and high purity cesium distillation.

The diode exhaust assembly of SN109CA is completed and is illustrated in Fig. 21. To complete the diode assembly the following welds were made: Two (2) seal subassembly to emitter support structures, two (2) seal assembly to collector-radiator subassembly, two (2) emitter to emitter support structures, three (3) alignment pin closures, and the reservoir subassembly to the collector-radiator subassembly.

All electron beam welds were checked leak tight on a 2 x 10^{-10} cc-atm/sec sensitive leak detector.

The diode assembly was thermal cycled to anticipated operating temperatures and all welds retained their mechanical and vacuum tight integrity.

SN109CA is now ready for cesium distillation and testing.

106844

Figure 21. SN109CA Diode Assembly

REFERENCES

1. A. E. Campbell, High-Performance Thermionic Converters, Contract 951225 9/2/66.

2. A. E. Campbell and D. L. Jacobson, Thermionic Research and Development Program, Contract NAS7-514, March 1, 1968.

3. Cleveland Refractory Metals, Technical Properties Data, Rhenium and Rhenium Alloys.

4. J. B. Conway and A. C. Losekamp, Thermal-Expansion Characteristics of Several Refractory Metals to 2500°C. Transactions of the Metallurgical Society of AIME, 702 - Volume 236, May 1966.

5. D. L. Jacobson, R. Hamerdinger, A. Campbell, First Quarterly Progress Report (4006-Q-1), Thermionic Research and Development Program, Contract NAS7-514, 12 July 1968.

APPENDIX A

ADDENDUM TO EOS REPORT 4006-Q-1

TABLE III

Change EOS Vacuum Emission vehicle measurements at 1953°K and 1903°K to read (Polished and Etched) rather than (Scribed).

TABLE VI

Correct as follows:

EFFECTIVE WORK FUNCTION ϕeff* FOR RHENIUM SINGLE CRYSTAL SAMPLE NO. I AND II FROM VACUUM EMISSION VEHICLE MEASUREMENTS

T°K	Fine Polish (I)	Fine Polish Electroetch (II)	Fine Polish Electropolish (I)
2003	5.05	5.04	5.06
2073	--	5.08	5.06
2101	5.08	5.08	5.05
2153	5.08	5.08	5.07
2217	5.13	--	--

* Estimated ϕeff ±0.04 e.v.

Figures 2-16, 2-17 and 2-18 are Schottky plots corresponding to the data of Table VI and are the corrected curves for the same numbered curves in EOS Report 4006-Q-1.

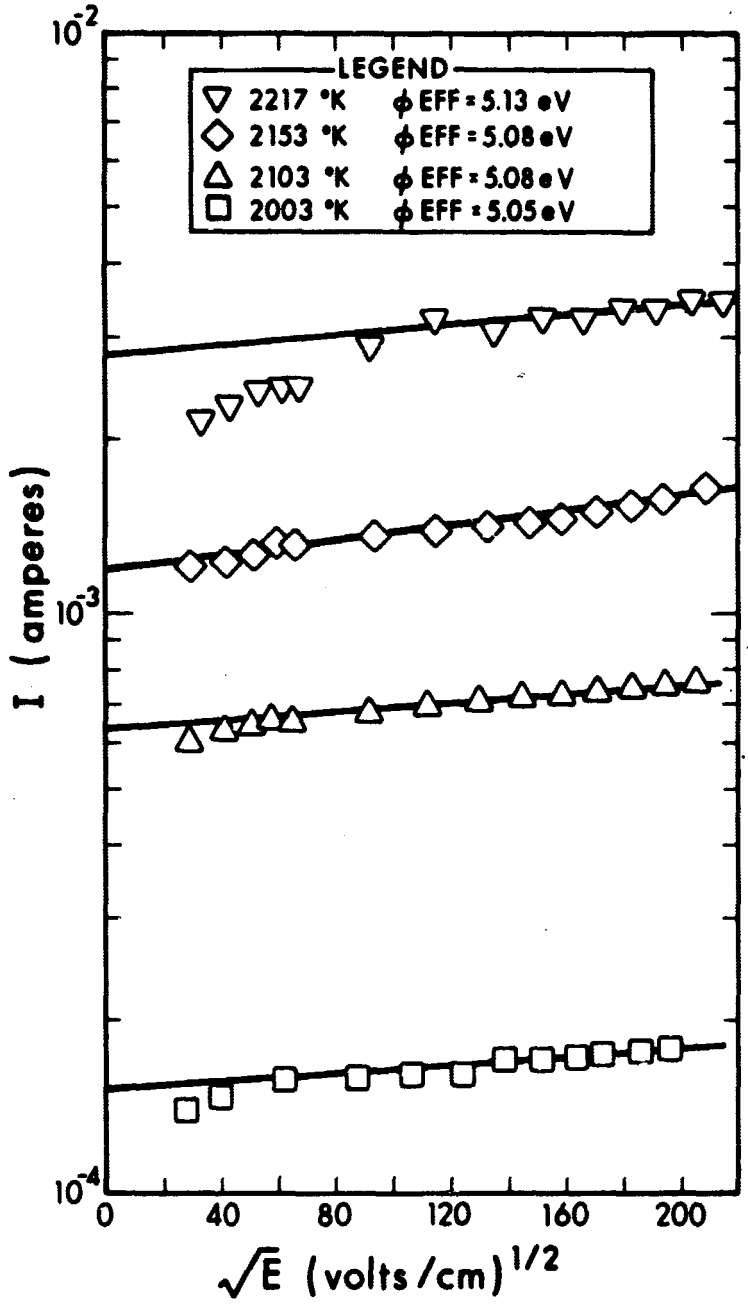

Figure 2-16. Schottky Plots of Single Crystal Rhenium Sample I (polished and high-fired for 2 hours at 2150°K)

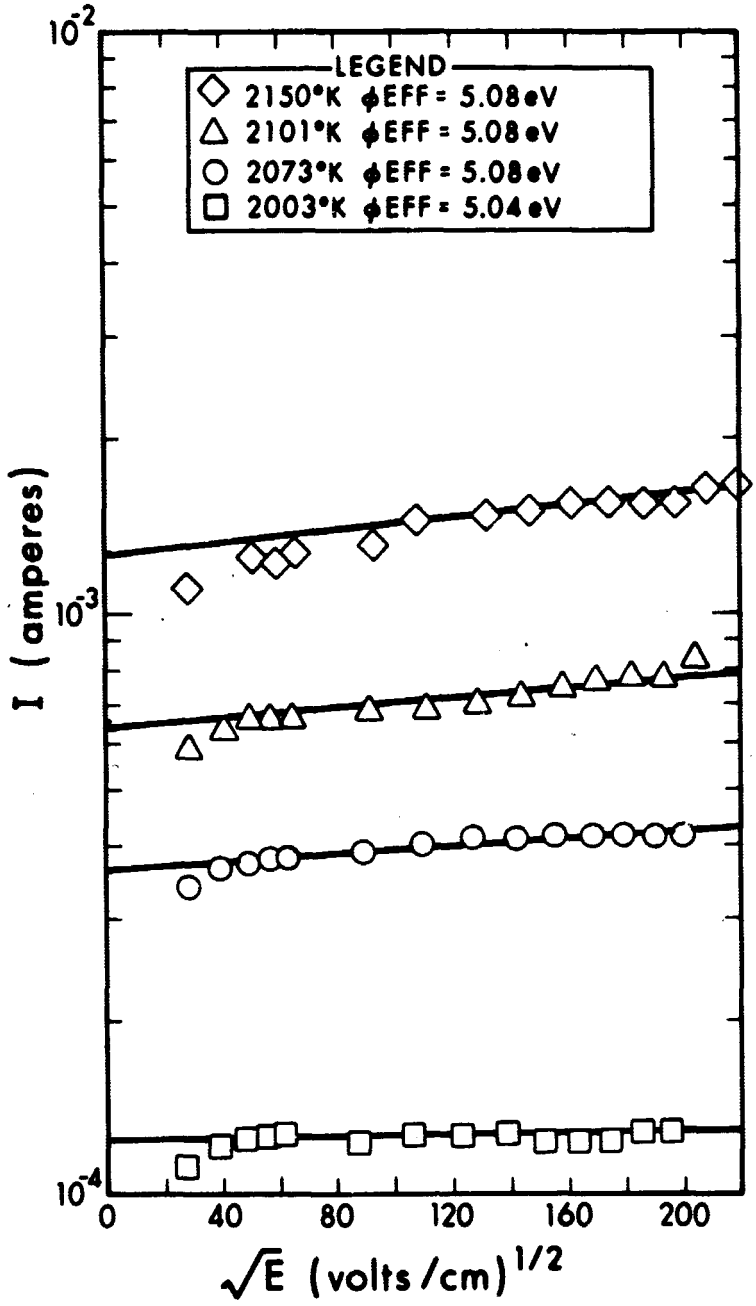

Figure 2-17. Schottky Plots of Single Crystal Rhenium Sample II (polished, electro-etched, and high-fired for 2 hours at 2150°K)

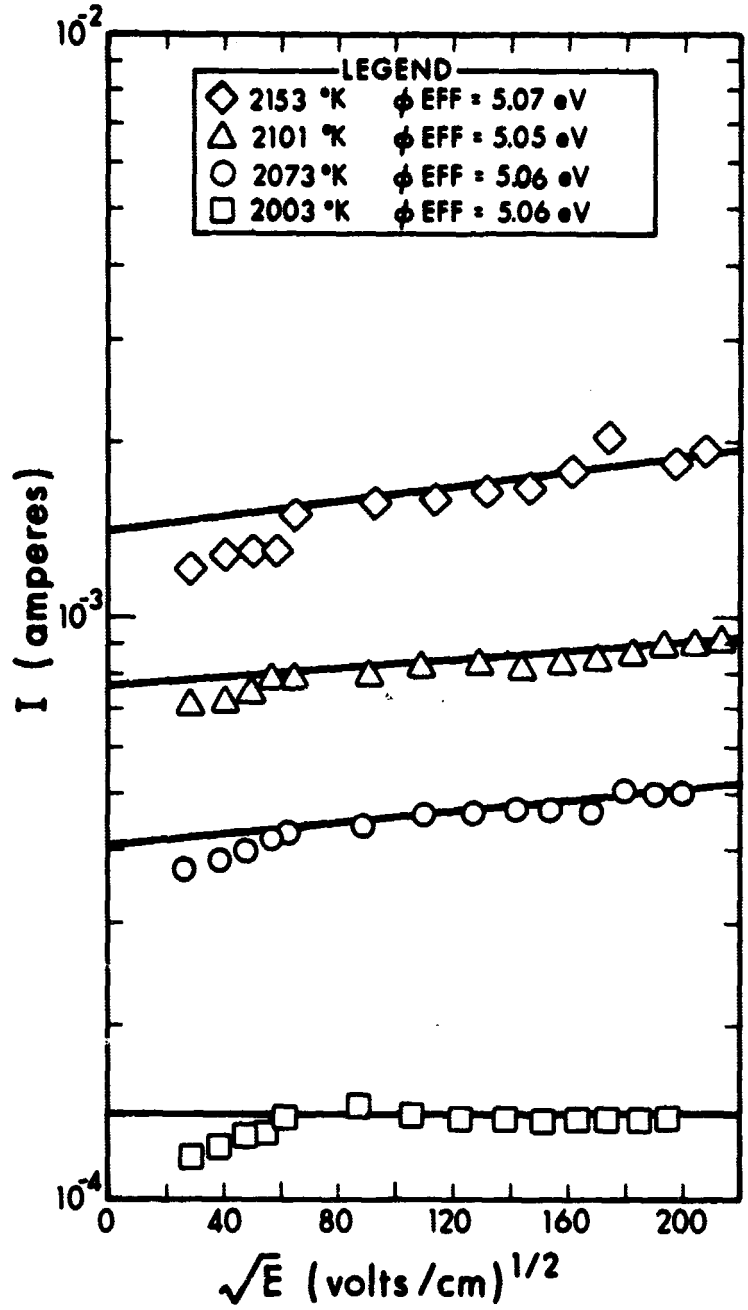

Figure 2-18. Schottky Plot of Single Crystal Rhenium Sample I (electropolished and high-fired for 1 hour at 2150°K)